

PERFORMANCE OF LOCAL AGGREGATE IN HIGH FRICTION SURFACE TREATMENT

by

HUMAIRA ZAHIR

B.S., Bangladesh University of Engineering and Technology, 2011

A THESIS

submitted in partial fulfillment of the requirements for the degree

MASTER OF SCIENCE

Department of Civil Engineering  
College of Engineering

KANSAS STATE UNIVERSITY  
Manhattan, Kansas

2016

Approved by:

Major Professor  
Dr. Mustaque Hossain

## **Abstract**

Road surfaces may prematurely lose pavement friction due to polished aggregates on sharp horizontal curves, steep grades, or near intersections resulting in vehicle skidding. The problem gets exacerbated during wet weather. The Federal Highway Administration (FHWA) estimates that about 70% of wet pavement crashes can be prevented or minimized by improving pavement friction. High Friction Surface Treatment (HFST), a specially-designed thin surface application of hard aggregates and thermosetting resins like epoxy, has been proven to be an effective method to increase road surface friction.

Calcined bauxite has been predominantly used in the United States as the hard aggregate in combination with an epoxy binder for HFST. However, this treatment is expensive since the calcined bauxite is imported. The objective of this study is to evaluate the performance of a local aggregate in HFST. Slab specimens of hot-mix asphalt (HMA) were compacted in the laboratory and treated with HFST systems incorporating both calcined bauxite and a local, hard aggregate, Picher Oklahoma flint aggregate. The treated HMA specimens were then tested with a Dynamic Friction Tester (DFT) and a Circular Track Meter (CTM) to determine the frictional coefficient and texture depth, respectively. Also, Hamburg Wheel Tracking Device Testing were conducted on these HFST systems to evaluate wearing resistance under repetitive wheel load. Field measurements of texture depths on HFST were also done. Statistical analysis was performed to compare the performance of high friction surfaces prepared with different aggregate epoxy combinations. The results show that flint aggregate can be a suitable substitute for the calcined bauxite in HFST. Field measurements also showed marked improvements in texture depth with HFST.

# Table of Contents

List of Figures .....	vi
List of Tables .....	viii
Acknowledgements .....	ix
Dedication .....	x
Chapter 1 - Introduction .....	1
1.1 General .....	1
1.2 High Friction Surface Treatment .....	2
1.3 Problem Statement .....	5
1.4 Objectives .....	7
1.5 Organization of Thesis .....	7
Chapter 2 - Literature Review .....	8
2.1 Background .....	8
2.2 High Friction Surface Treatment Process .....	8
2.3 Commonly Used Aggregates for HFST .....	10
2.3.1 Calcined bauxite aggregate .....	11
2.3.2 Dolomite aggregate .....	12
2.3.3 Granite aggregate .....	13
2.3.4 Silica sand .....	13
2.3.5 Steel slag .....	14
2.3.6 Flint aggregate .....	15
2.4 Binders for High Friction Surface Treatment .....	15
2.4.1 Epoxy resin .....	16
2.4.2 Rosin ester .....	16
2.4.3 Polyurethane resin .....	16
2.4.4 Acrylic resin .....	17
2.5 HFST Application Procedure .....	17
2.5.1 General application procedure .....	17
2.5.2 Precautions for HFST application on concrete surface .....	19
2.5.3 Precautions for HFST application on asphalt surface .....	20

2.5.4 Precautions for HFST application on an open graded friction course .....	20
2.6 Benefits of HFST Process .....	20
2.7 HFST Compared to Microsurfacing Treatment .....	24
2.8 Causes of failure of HFST .....	25
2.9 Unit Cost of HFST .....	26
2.10 HFST projects in Kansas .....	27
2.11 Summary .....	35
Chapter 3 - Methodology .....	36
3.1 Field Tests .....	36
3.1.1 Laser Crack Measurement System .....	36
3.1.2 Locked Wheel Skid Trailer .....	37
3.2 Laboratory Tests .....	38
3.2.1 Experimental Design .....	38
3.2.2 Aggregate Tests .....	38
3.2.2.1 Aggregate gradation test .....	40
3.2.2.2 Specific gravity test .....	42
3.2.2.3 Moisture content test .....	43
3.2.2.4 Fine aggregate angularity test .....	45
3.2.2.5 Sand equivalent test .....	46
3.2.2.6 Aggregate durability index test .....	48
3.2.3 Preparation of Slab Specimen .....	49
3.2.4 Epoxy Application .....	50
3.2.5 High Friction Surface Preparation .....	51
3.2.6 Tests performed on Prepared High Friction Surfaces .....	54
3.2.6.1 Testing with a circular track meter .....	54
3.2.6.2 Testing with a dynamic friction tester .....	56
3.2.6.3 Testing with a Hamburg Wheel Tracking Device .....	58
Chapter 4 - Results and Discussion .....	59
4.1 Field Test Results .....	59
4.1.1 K-18 westbound and I-70 westbound on-ramp .....	59
4.1.2 K-177 southbound and I-70 westbound on-ramp .....	60

4.1.3 I-70 westbound and K-177 northbound off-ramp .....	60
4.1.4 K-5 roadway with high friction surface .....	62
4.1.5 Relationship between Texture depth and Skid number .....	62
4.2 Laboratory Test Results .....	63
4.2.1 Aggregate test results .....	63
4.2.1.1 Aggregate gradation test result .....	63
4.2.1.2 Specific gravity test results .....	66
4.2.1.3 Moisture content test results .....	66
4.2.1.4 Fine aggregate angularity test results.....	66
4.2.1.5 Sand equivalent test result .....	67
4.2.1.6 Durability index test result.....	67
4.2.2 Test Results of Prepared High-Friction Surfaces.....	67
4.2.2.1 Bauxite Aggregate-Mark-154 Epoxy Combination.....	68
4.2.2.2 Flint Aggregate-Mark-154 Epoxy Combination.....	69
4.2.2.3 Bauxite Aggregate-Pro-Poxy Type III Epoxy Combination .....	71
4.2.3 Statistical Analysis.....	72
Chapter 5 - Conclusions and Recommendations .....	76
5.1 Conclusions.....	76
5.2 Recommendations.....	78
References.....	79

## List of Figures

Figure 1.1 Pavement with HFST (left) and conventional pavement (right) (Stoikes, 2014).....	3
Figure 1.2 Relationship between pavement friction and crash risk (Viner et al., 2005) .....	4
Figure 1.3 National use of HFST (HFST overview, FDOT, 2015) .....	5
Figure 2.1 Hot-applied HFST (High Friction Surfaces, 2014) .....	9
Figure 2.2 Cold-applied HFST (Hill, 2015).....	10
Figure 2.3 Calcined bauxite aggregate.....	12
Figure 2.4 Dolomite aggregate .....	12
Figure 2.5 Granite aggregate.....	13
Figure 2.6 Silica sand.....	14
Figure 2.7 Steel slag.....	14
Figure 2.8 Flint aggregate .....	15
Figure 2.9 HFST manual application (HFST overview, FDOT, 2015).....	18
Figure 2.10 HFST semi-automated application (HFST overview, FDOT, 2015) .....	18
Figure 2.11 HFST fully automated application (HFST overview, FDOT, 2015).....	19
Figure 2.12 HFST crash reduction effectiveness (Mills, 2015).....	23
Figure 2.13 Stopping distance reduction in HFST (LeFante, 2015).....	24
Figure 2.14 Typical Microsurfacing Treatment (Micro Surfacing, 2015).....	25
Figure 2.15 HFST locations in Kansas: K-99, K-5, K-96/US-54, I-35/I-635 (clockwise from top left).....	28
Figure 2.16 Before and after HFST on K-99 in Wabaunsee County (asphalt pavement) .....	29
Figure 2.17 Before and after HFST on K-5 in Leavenworth County (asphalt pavement).....	30
Figure 2.18 Before and after HFST on I-35/I-635 ramp in Kansas City (concrete pavement) ....	31
Figure 2.19 Before and after HFST on K-96/US-54 ramp in Wichita (concrete pavement).....	31
Figure 2.20 HFST locations on K-177 (left) and K-18 (right) .....	32
Figure 2.21 De-bonding of high friction surface aggregates .....	33
Figure 2.22 K-7/K-10 interchange loop ramp.....	34
Figure 3.1 KDOT Laser Crack Measurement System used in this study .....	37
Figure 3.2 Locked Wheel Skid Trailer data collection .....	37
Figure 3.3 Chinese calcined bauxite aggregate used in this study.....	38

Figure 3.4 Pitcher, Oklahoma flint aggregate used in this study .....	40
Figure 3.5 Aggregate sample reduction using quartering method .....	41
Figure 3.6 Moist flint (left) and clean flint (right) aggregate .....	44
Figure 3.7 Experimental setup of fine aggregate angularity test .....	45
Figure 3.8 Siphon assembly with irrigator tube .....	47
Figure 3.9 Sand and clay reading in sand equivalent test .....	48
Figure 3.10 Compacted slab in kneading slab compactor .....	50
Figure 3.11 Jiffy mixer used for epoxy mixing .....	50
Figure 3.12 Mixing of part A and B of the epoxy .....	51
Figure 3.13 Duct tape applied on sides of the slab to prevent epoxy loss .....	52
Figure 3.14 Epoxy application over the slab .....	53
Figure 3.15 Slab covered with epoxy .....	53
Figure 3.16 Aggregate is being spread over the epoxy covered slab.....	54
Figure 3.17 Circular track meter for measuring texture depth.....	55
Figure 3.18 Rubber sliders fitted in the bottom of DFT .....	56
Figure 3.19 Dynamic friction tester for measuring frictional coefficient.....	57
Figure 3.20 Hamburg Wheel Tracking Device.....	58
Figure 4.1 Texture depth values along K-18/I-70 on-ramp .....	59
Figure 4.2 Texture depth values along K-177/I-70 on-ramp .....	60
Figure 4.3 Texture depth values along I-70/K-177 off-ramp .....	61
Figure 4.4 De-bonding of high friction surfaces.....	61
Figure 4.5 Relationship between texture depth and skid (using Grooved tire) .....	62
Figure 4.6 Relationship between texture depth and skid (using Smooth tire) .....	63
Figure 4.7 Gradation curve of bauxite aggregate.....	65
Figure 4.8 Gradation curve of flint aggregate.....	65
Figure 4.9 Texture depth of combination 1 .....	68
Figure 4.10 Improved FN of HFSs prepared with combination 1 .....	69
Figure 4.11 Texture depth of combination 2 .....	70
Figure 4.12 Improved FN of HFSs prepared with combination 2 .....	70
Figure 4.13 Texture depth of combination 3 .....	71
Figure 4.14 Texture depth of combination 4 .....	72

## List of Tables

Table 1.1 Relationship between Frictional co-efficient and Crash rate (Wallman and Astrom, 2001) .....	2
Table 2.1 Aggregate properties for HFST (KDOT, 2007).....	11
Table 2.2 Aggregate Grading (KDOT, 2007).....	11
Table 2.3 Epoxy resin properties for HFST (KDOT, 2007).....	16
Table 2.4 Summary statistics of HFST treatment sites (Merritt et al., 2015).....	21
Table 2.5 Hypothetical scenarios of crash reductions and economic benefits (Mills, 2015) .....	22
Table 3.1 Chemical composition of calcined bauxite aggregate (Great Lake Minerals).....	39
Table 3.2 Physical properties of calcined bauxite aggregate (Great Lake Minerals, LLC.).....	39
Table 3.3 Material properties of the epoxy used.....	51
Table 4.1 Aggregate gradation test results of bauxite aggregate .....	64
Table 4.2 Aggregate gradation test results of bauxite aggregate .....	64
Table 4.3 Bulk specific gravity of bauxite and flint aggregate.....	66
Table 4.4 Two-way factorial analysis result .....	75



## **Acknowledgements**

First, I would like to pay my utmost respect to Almighty for granting me this wonderful opportunity. I hereby acknowledge my gratefulness to my major professor, Dr. Mustaque Hossain, for his academic guidance and perennial support to me. I am very thankful to Dr. Robert Stokes and Dr. Sunanda Dissanayake for being part of my thesis committee and all their suggestions for making my thesis better.

I appreciate the financial support from the Kansas Department of Transportation for completing this research work. I am very thankful to my graduate colleagues and undergraduate assistants for helping me during this research work.

Finally, I would like to specially thank my family members for their encouragement, patience and support.

## **Dedication**

I would like to dedicate this thesis to my beloved family members whose affection, love, encouragement, and prayers make me achieve this success and honor.

# **Chapter 1 - Introduction**

## **1.1 General**

High quality pavement is an essential prerequisite for safe highway condition. Friction, or resistance to skidding, helps determine existing pavement condition. Pavement surface friction is defined as a force that resists relative motion of a vehicle tire over a pavement surface; resistive force is generated as tires roll or slide over the pavement (Baron, 2015). An appropriate amount of pavement friction is necessary for safe driving conditions, especially to prevent roadway departure crashes such as run-off-road and head-on collisions. When pavement friction decreases, the road surface becomes polished, thereby increasing the possibility of a vehicle skidding around sharp horizontal curves, steep grades, or near an intersection. A polished road surface is a primary cause of highway fatalities; more than 10,000 fatal crashes occur throughout the United States each year due to substandard pavement conditions (Hall et al., 2009).

Number of fatal crashes increases when pavements are wet. Although the relationship between pavement friction and wet-weather crashes is difficult to compute precisely, research has shown that wet-weather crashes increase when pavement friction decreases (Hall et al., 2009). Wet pavement is a factor in approximately 25 percent of all crashes and 14 percent of all fatal crashes (Julian and Moler, 2008). The Federal Highway Administration (FHWA) has estimated that improved pavement surface friction can prevent approximately 70% of wet-weather crashes. A comprehensive evaluation of friction measurements and crash rates revealed that increasing pavement friction significantly reduces crash rates (Wallman and Astrom, 2001), as summarized in Table 1.1:

**Table 1.1 Relationship between Frictional co-efficient and Crash rate (Wallman and Astrom, 2001)**

<b>Frictional Coefficient</b>	<b>Crash Rate (injuries per million vehicle km)</b>
<0.15	0.80
0.15–0.24	0.55
0.25–0.34	0.25
0.35–0.44	0.20

## **1.2 High Friction Surface Treatment**

Vehicle speed and roadway geometry often create a friction demand that cannot be achieved with standard pavement surfaces. However, high friction surface can resolve this demand for high friction. High Friction Surface Treatment (HFST) is a specially designed process that can dramatically and immediately reduce crashes and fatalities (Viner et al., 2005). In HFST, a thermosetting polymer resin binder or epoxy is sprayed on the existing pavement surface and then hard, durable aggregates are spread on top of the epoxy layer. The resin binder locks the aggregates firmly in place, producing a durable surface with high friction. HFST can restore pavement surface friction characteristics at locations in which traffic has polished existing pavement surface aggregates. HFST also successfully compensates for inadequate roadway geometric designs such as abrupt curves and variable superelevations. Figure 1.1 shows a pavement with HFST (on the left) and a conventional pavement (on the right). From the figure it is clear that a conventional pavement is more smooth and polished than a high friction surface.



**Figure 1.1 Pavement with HFST (left) and conventional pavement (right) (Stoikes, 2014)**

In locations with gradual friction reduction, vehicle skidding occurs when drivers abruptly brake, turn, or speed up their vehicles. Although road markings and signs aid cautious drivers, excessive vehicle speed is a major contributing factor to roadway crashes, especially near curves. Vehicles occasionally enter curves at high speeds, decreasing the ability to control vehicle skidding. Overcoming crash risks on sharp curves requires additional friction to keep vehicles on the roadway, thereby necessitating further polishing of pavement surface aggregates. HFST enhances pavement friction of critical maneuver locations and ensures increased safety, advantageously assisting drivers. Studies have shown that crash risk significantly decreases as pavement friction doubles as shown in Figure 1.2 (Viner et al., 2005).

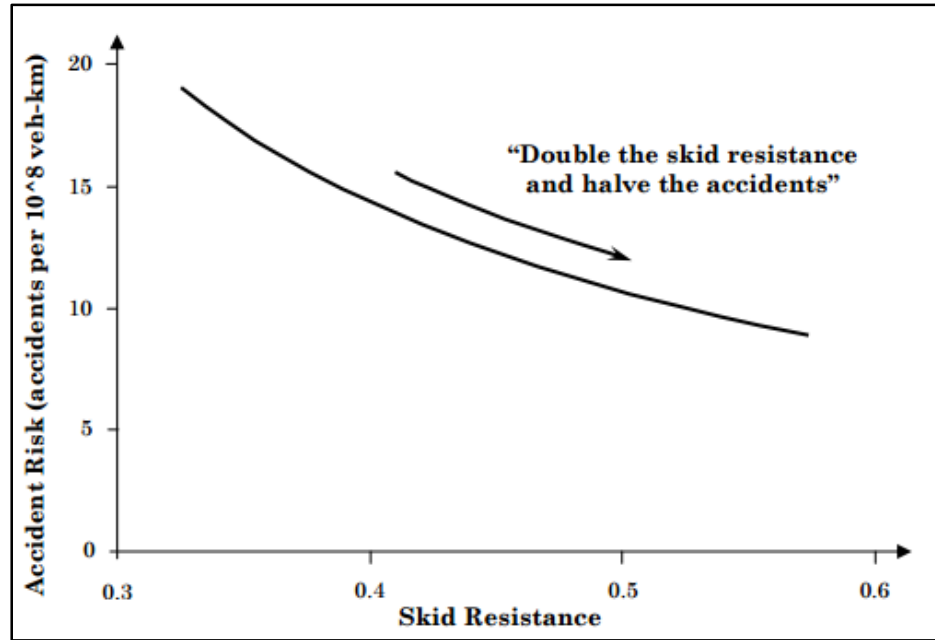


**Figure 1.2 Relationship between pavement friction and crash risk (Viner et al., 2005)**

HFSTs are typically installed in single or double layers at roadway locations where drivers begin to brake. Brake lights near horizontal curves usually indicate where HFST application should start since the goal of HFST is to reduce vehicle speed entering a curve. Most states end treatment at a point of tangent (Brimley and Carlson, 2012). Motorists may notice an irregular riding surface in treated areas, but they also experience extra pavement friction, resulting in improved control of their vehicles. Friction improvement projects are using HFST because this treatment is cost-effective, and the products used for treatment have negligible environmental impacts. National use of HFST is shown in Figure 1.3.

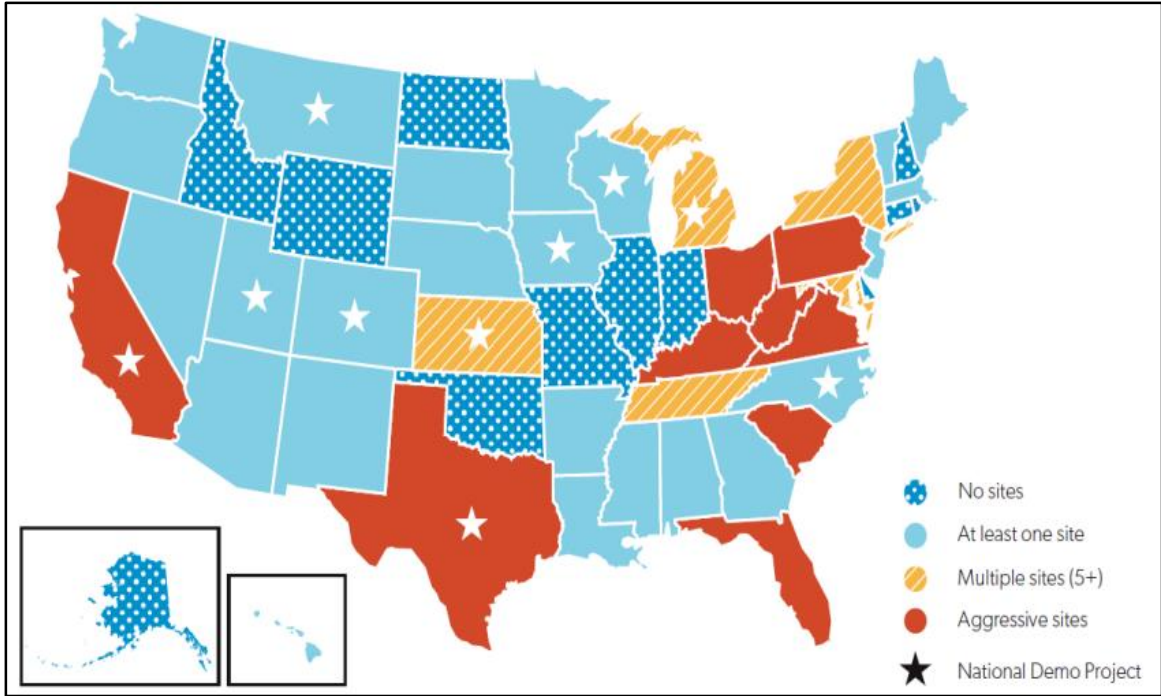


**Figure 1.3 National use of HFST (HFST overview, FDOT, 2015)**

### **1.3 Problem Statement**

This project is divided into two major parts: a) to determine the field performance of HFST and b) to compare performance of a manufactured and a local aggregate in HFST in the laboratory. In the field, a Locked Wheel Skid Trailer (LWST) is universally used to determine road surface friction characteristics. LWST measures pavement skid numbers. The driving speed of a vehicle should be 40 miles per hour (mph) for skid number determination, but maintaining constant speed is difficult, especially on curves and ramps (Flintsch et al., 2009). However, because pavement surface friction is a function of surface texture, estimation of texture characteristics could provide useful information about the frictional condition of the roadway. Surface texture provides a gritty surface that allows a thin water film to penetrate into the pavement and produces satisfactory frictional resistance between tires and pavement (McGhee et al., 2003). A two-dimensional (2-D) profiler measures the texture profile with distance along the pavement surface as one dimension

and texture elevation as the second dimension. A three-dimensional (3-D) profiler more precisely measures pavement texture compared to a 2-D profiler that fails to completely describe pavement texture characteristics. Texture depth of pavement or the Mean texture depth (MTD) are generally calculated to estimate average vertical height of the pavement surface texture. Although the sand patch test method is most commonly used to determine MTD of pavement surfaces (Brown et al., 2002), Laser Crack Measurement System (LCMS) is more precise and safer to use to measure surface texture depth because it can be operated at posted highway speeds without interrupting the flow of traffic (Laurent et al., 2008). So, in order to compare the field performances of HFST, a LWST and a LCMS were used and skid numbers and texture depths were determined and compared.

Aggregates such as bauxite, flint, granite, basalt, silica, steel slag, and occasionally, glass beads are commonly used for HFST projects. Calcined bauxite, a manufactured aggregate, has been predominantly used for HFST projects because it has a high polished stone value (PSV), generally exceeding 70, and wear resistance. PSV is determined via a laboratory test that measures aggregate friction after wear from an abrasive wheel. Aggregates with PSV value over 60 are high friction aggregates. Although the calcination process increases aggregate hardness and stability, the process increases aggregate cost: Bauxite aggregates are generally \$350–\$500 per ton compared to \$20–\$30 for local aggregates. Thus use of local aggregates instead of calcined bauxite can lower project costs by reducing aggregate manufacturing and transportation costs. So, in the laboratory, widely used bauxite aggregate and local flint aggregate were used to prepare high friction surfaces and their performances were compared. In order to compare HFST performances, two pieces of equipment were used in the laboratory; Circular Track Meter (CTM)) was used to measure texture depth of high friction surfaces and Dynamic Friction Tester (DFT) was used to



identify the frictional co-efficient of the surface. As the prepared high friction surfaces in the laboratory were smaller in dimension (32cm x 26cm) than a roadway segment, CTM and DFT were used in the lab instead of LCMS and LWST.

## **1.4 Objectives**

This study contained the following objectives:

- a) To investigate friction number progression on selected HFST projects in Kansas
- b) Determine bauxite and flint aggregate quality and compliance with current specification of HFST
- c) Observe skid improvement using local flint aggregate in HFST
- d) Evaluate wearing resistance and bonding between high friction aggregate and epoxy, and
- e) Compare texture depth and friction resistance of bauxite and flint aggregates.

## **1.5 Organization of Thesis**

This thesis is divided into five chapters. Chapter 1 contains an introduction to HFST, the problem statement, and study objectives. Chapter 2 includes a literature review related to the HFST process, including descriptions of high friction aggregates and epoxy binders, a review of existing HFST pavements, benefits of the HFST process, and how this process differs from other microsurfacing treatment. Chapter 3 discusses high friction surface simulation including aggregate tests, HFST design and laboratory test methods, and tests performed in laboratory and field. Chapter 4 includes aggregate test results, test results performed on high friction surfaces and statistical analysis of results. Chapter 5 concludes this study and presents recommendations for further study.

## **Chapter 2 - Literature Review**

### **2.1 Background**

In the United States, one person dies every 12 minutes in motor vehicle crashes (Julian and Moler, 2008). Several previous studies established that friction or anti-skidding characteristic of pavement surface is a dominant factor for controlling and reducing highway crashes. Keeping that in mind, techniques for improving pavement friction are receiving increased attention in pavement management processes now a days. HFST or pavement surface friction improvement treatment technology originated in 1950s. At that time U.K. government's Transportation and Road Research Laboratory (TRRL) initiated testing of various hard aggregates and binder combinations to construct extremely high friction surfaces (Nicholls, 1998). Later in 1980s, some researchers from the United States started testing the efficiency of these surfaces to reduce skidding or polished pavement surface related crashes. In 1989, the University of Michigan conducted a survey for the Federal Highway Administration (FHWA) on 15 ramps at 11 interchanges in five states. According to the researchers, surface properties of those places were related to roadway geometry and vehicle dynamics (Julian and Moler, 2008). At present, more studies are going on for better understanding the HFST process, the behavior of different friction testing devices, and the influence of texture, speed, and other external conditions on their measurements.

### **2.2 High Friction Surface Treatment Process**

HFST application can be categorized as hot-applied high friction surfacing or cold-applied high friction surfacing (Nicholls, 1997). Thermoplastic resin, which is used in hot applied high friction surfacing, becomes liquid when heated and solid when cooled to ambient temperature. In hot-applied high friction surfacing, high friction aggregate and resin are heated thermostatically

and applied to the surface while hot (Figure 2.1). This system is not weather dependent, and treated road segments can be opened to traffic within 15 minutes of material application. Overheating of the high friction material, however, can decrease this system's durability.



**Figure 2.1 Hot-applied HFST (High Friction Surfaces, 2014)**

In cold-applied high friction surfacing, epoxy or polyurethane-based resins must be spread within a certain period of time (depending on the workplace temperature) after mixing due to initiation of a heat-producing chemical reaction that results in hardening of the resin. The required amount of aggregate is then applied over the resin (Figure 2.2), requiring a few hours (based on the workplace temperature) to set completely.



**Figure 2.2 Cold-applied HFST (Hill, 2015)**

### **2.3 Commonly Used Aggregates for HFST**

All high friction surfaces consist of two main components, aggregate and binder. Hard, durable aggregates capable of providing long-lasting, skid-resistant surfaces are commonly used for HFST. These aggregates must resist degradation (evaluated by ASTM C131), polishing (evaluated by ASTM D3319), and freeze-thaw damages. Aggregates should also have a high PSV in order to provide sufficient friction when used in road surfacing; a treated surface layer must preserve its texture for as long as possible to provide adequate skid resistance. As mentioned in Chapter 1, commonly used aggregates for HFST include calcined bauxite, dolomite, granite, silica, steel slag, and flint. Required aggregate properties and gradation for HFST are specified in Tables 2.1 and 2.2.

**Table 2.1 Aggregate properties for HFST (KDOT, 2007)**

<b>Property</b>	<b>Requirements</b>	<b>Test Method</b>
Polishne Value	38, minimum	AASHTO T-279
Wear	20 %, maximum	AASHTO T-96, Grading D
Moisture Content	0.2 %, maximum	KT-11
Fine Aggregate Angularity	45 %, minimum	AASHTO T-304, Method A
Freeze-Thaw Soundness	9 %, maximum	AASHTO T-103

**Table 2.2 Aggregate Grading (KDOT, 2007)**

<b>Sieve Size</b>	<b>% Retained by weight</b>
No. 4	0
No. 8	0–5
No. 16	95–100
No. 30	99–100
No. 50	99–100
No. 100	99–100

### **2.3.1 Calcined bauxite aggregate**

Bauxite undergoes calcination process, in which the aggregate is collected from aluminium ore and exposed to prolonged heating at an elevated temperature of approximately 1600 °C to increase its physical stability and hardness. Depending on the source of bauxite aggregate, its density varies from 2.6 to 3.4 g/cm<sup>3</sup> (Izeppi et al., 2010). Typical PSVs of calcined bauxite range from 60 to 70; density is a good indicator of PSV (i.e., high density usually indicates high PSV). A picture of calcined bauxite aggregate is shown in the Figure 2.3 below.



**Figure 2.3 Calcined bauxite aggregate**

### **2.3.2 Dolomite aggregate**

Some HFSTs include aggregates largely comprised of mineral dolomite. Dolomite is commonly light in color, and traces of iron in this mineral give it a yellow or brown tint. Dolomite is the double carbonate of calcium and magnesium in which a portion of the calcium from limestone is replaced by magnesium. The replacement is seldom complete, however, and many grades exist between limestone and dolomite (Huhta et al., 2001). Figure 2.4 is showing the dolomite aggregates used for high friction surface treatment.



**Figure 2.4 Dolomite aggregate**

### **2.3.3 Granite aggregate**

Granite aggregate generally consists of quartz and potassium feldspar. This aggregate varies in color from very light to medium tones of gray, as shown in Figure 2.5. Due to its mineral composition and interlocking crystals, granite is hard and abrasion resistant: Compressive strength of granite is usually above 200 MPa, and it is harder than sandstone, limestone, or marble. The average density of granite is between 2.65 and 2.75 g/cm<sup>3</sup>, and it shows PSVs of 62 or greater (Huhta et al., 2001).



**Figure 2.5 Granite aggregate**

### **2.3.4 Silica sand**

Silica naturally occurs in abundance as sandstone, silica sand, or quartzite in an amorphous form (vitreous silica) or a variety of crystalline forms. Silica has high abrasion resistance and thermal stability. Three crystalline forms of silica are quartz, tridymite, and cristobalite, with high and low variations of each. Silica has high thermal expansion that can cause casting defects with high melting point metals, and its low thermal conductivity can lead to unsound casting. Silica is insoluble in all acids except hydrogen fluoride (Rao, 2003). Figure 2.6 is representing a silica sand sample used for high friction surface treatment.



**Figure 2.6 Silica sand**

### **2.3.5 Steel slag**

Slag is a by-product of steel manufacturing that is produced when molten steel is separated from impurities in the blast furnaces. Slag forms as a molten liquid melt, and is a complex solution of silicates and oxides that solidifies upon cooling. Steel slag must be crushed and screened (Figure 2.7) to produce a suitable aggregate for an HFST system (Shi, 2004).



**Figure 2.7 Steel slag**



### **2.3.6 Flint aggregate**

Flint aggregate is a variety of chert, a fine-grained silica-rich sedimentary rock. During the geological process of diagenesis, chemical changes occur in the compressed sedimentary rock, resulting in flint aggregates. This aggregate is dark grey with shades of brown, red, or yellow, and sometimes white (Figure 2.8). Flint is hard and tends to split into pieces that have curved but even surfaces (Sorrell, 1973).



**Figure 2.8 Flint aggregate**

## **2.4 Binders for High Friction Surface Treatment**

Resinous binders such as epoxy resin, rosin ester, polyurethane resin, and acrylic resin are currently used in HFST systems (Nicholls, 1998). Epoxy resins should meet requirements listed in Table 2.3.

**Table 2.3 Epoxy resin properties for HFST (KDOT, 2007)**

<b>Property</b>	<b>Requirements</b>	<b>Test Method</b>
Viscosity	1000–2500 cps	ASTM D 2196
Gel Time	15–45 minutes	ASTM C 811, para. 11.2.1
Compressive Strength, 3h	1000 psi, min	ASTM C 579, Method B*
Compressive Strength, 24 h	5000 psi, min	ASTM C 579, Method B*
Tensile Strength, 7 days	2000–5000 psi	ASTM D 638, Type 1
Elongation (neat), 7 days	30–80 percent	ASTM D 638, Type 1
Chloride Ion Penetration	100 coulombs, max	AASHTO T 277

### **2.4.1 Epoxy resin**

Epoxy resin, which has the longest history of use in HFST systems, consists of a two-component system mixed in-situ at 50:50 by volume. One component contains the resin with a portion of oils that reduce resin viscosity to allow flow (extender); the other component contains the curing agent (hardener). Although binder properties can be adjusted by changing proportions of the system components, typical curing times range between 3 and 4 hours for applications at pavement temperatures greater than 10 °C.

### **2.4.2 Rosin ester**

Rosin ester is a pre-blended system that facilitates in-situ installation operations. It can readily be heated at a specified temperature and placed on the surface. A handheld box is used for application, resulting in an approximate thickness of 5 mm that stiffens quickly due to thermos-plasticity. Use of rosin ester allows possible early opening to traffic compared to other resins.

### **2.4.3 Polyurethane resin**

Use of polyurethane resin results in less curing time at lower temperatures compared to other resins. This binder is a chemically curing, multiple-component system that is mixed with a

handheld beater and laid manually. Aggregate is then manually or mechanically spread separately on top of the resin.

#### **2.4.4 Acrylic resin**

Acrylic resin is a two-component system with a much faster curing time than epoxy resin. The curing process, however, does not begin until aggregates containing the curing agent are spread over the resinous surface. Binder consistency is designed to sufficiently wet the aggregates in order to provide an adequate bond without the binder flooding the crushed stone/aggregate particles or chips.

### **2.5 HFST Application Procedure**

#### **2.5.1 General application procedure**

Areas recommended for HFST include bridge decks, intersections, roundabouts, toll plazas, bus lanes, exit-entrance ramps, crosswalks, school crossings, corners, steep grades, horizontal curves, and other identified skid hazardous areas (Izeppi et al., 2010). Prior to treatment, existing travelled surfaces must be dry, clean, and free from ice, frost, loose aggregates, oil, grease, road salt, and other loose matters likely to impede aggregate binder adhesion. Cleaning of the surface is accomplished using brooms, compressed air, and/or shot blasting. The surface temperature should be measured to verify that it meets the installation standard, and drains, joints, and expansion devices must be covered with duct tape and plastic to prevent clogging from epoxy and aggregates.

Epoxy-aggregate application can occur as manual application, semi-automated application, and fully automated application. The epoxy usually consists of part A and part B. In the manual method, both parts are mixed manually using a slow-speed drill fitted with a helical mixing blade.

Aggregates are distributed manually immediately following binder spreading. After a certain curing time (based on the workplace temperature), excess or loose aggregates are removed from the surface using a brush (Figure 2.9). Production rate in this method varies from 160 to 400 m<sup>2</sup>/hr.



**Figure 2.9 HFST manual application (HFST overview, FDOT, 2015)**

In the semi-automated method, machine-aided broadcasting of aggregate is followed by machine mixing with hand application of the resin binder (Figure 2.10). The production rate in this process is up to 1,650 m<sup>2</sup>/hr. In the fully automated method (Figure 2.11), machines mix the resin and apply the resin and aggregates on the pavement surface. The production rate in the fully automated method can be up to 3,000 m<sup>2</sup>/hr.



**Figure 2.10 HFST semi-automated application (HFST overview, FDOT, 2015)**



**Figure 2.11 HFST fully automated application (HFST overview, FDOT, 2015)**

HFST application temperature varies depending on the type of resin/epoxy used. The recommended temperature range of HFST installation is 12-37 °C. Curing time typically varies from 2 to 4 hr for most applications under normal ambient temperatures (23 °C), although lower than normal ambient temperatures can increase curing time and potentially compromise long-term performance of HFST.

### **2.5.2 Precautions for HFST application on concrete surface**

Some precautions need to be taken when HFSTs are applied over concrete pavements. Polymer resin binder should not be used over Portland cement that was placed less than 28 days prior to HFST application. Surface patching and cleaning should be ensured before treatment. Prior to application, the concrete surface must be cleaned thoroughly by shot blasting or another abrasive method to remove oils, dirt, rubber, paint, weak surface mortar, and any potentially damaging waste products that may affect adhesion between binder and aggregate and system curing. If HFST is applied in double layer, both layers should be applied within 24 hours.

### **2.5.3 Precautions for HFST application on asphalt surface**

Precautions for HFST application on an asphalt surface are similar to the application on a concrete surface. Removal of contaminants from the existing surface/pavement is necessary before application. High pressure air or a vacuum, not a broom, is recommended to remove all dust and loose materials from the existing pavement. HFST application over new asphalt pavements should be applied no sooner than 30 days after paving.

### **2.5.4 Precautions for HFST application on an open graded friction course**

Open graded pavement surfaces no longer function as open graded surfaces after HFST installation. HFST application on an open graded friction course (OGFC) or grooved concrete surface may require two layers of application in order to seal voids and maintain proper binder depth. HFST application over OGFC may require the shoulder of the high side of superelevation to be sealed to prevent water from passing through the OGFC, potentially causing failure of HFST.

## **2.6 Benefits of HFST Process**

HFST distinctively resolves site-specific issues, improves friction on existing pavements and skid resistance on new pavements. Although, a majority of high friction demand locations are on local and collector systems, this treatment is also advantageous at high volume intersections, interchange ramps, and selected interstate alignment segments. Pennsylvania, Kentucky, and South Carolina Departments of Transportation (DOTs) have reported total crash reductions of 100%, 90%, and 57%, respectively, for their signature trial HFST application projects. The study period after application ranged from 3 to 5 years. Kentucky installed 60 HFST applications from years 2010–2012 and measured their performance. These sites showed a total crash reduction of

78%, with a wet weather crash reduction of 85% (Merritt et al., 2015). Table 2.4 summarizes the crash statistics before and after HFST process.

**Table 2.4 Summary statistics of HFST treatment sites (Merritt et al., 2015)**

<b>Site Type</b>	<b>Sites by state</b>	<b>Crashes/site (Before treatment)</b>	<b>Crashes/site (After treatment)</b>	<b>Wet crashes/site (Before treatment)</b>	<b>Wet crashes/site (Before treatment)</b>
Ramps	Kansas-2 Kentucky-2 Michigan-6 Montana-1 South Carolina-6 Wisconsin-1	Min-0.00 Max-28.68	Min-0.00 Max-10.50	Min-0.00 Max-12.25	Min-0.00 Max-3.00
Curves	Colorado-2 Kansas-2 Kentucky-28 Michigan-1 Montana-1 South Carolina-1 Tennessee-4	Min-0.25 Max-17.00	Min-0.00 Max-16.00	Min-0.00 Max-14.00	Min-0.00 Max-4.00

HFST processes result in a high benefit-cost ratio. South Carolina DOT installed a series of curves and reported a benefit-cost ratio of 24 to 1. On average, crashes in Kentucky decreased from 6.2 to 1.9 per year at curves treated with HFST. According to an FHWA report, Wisconsin demonstrated a 95% crash reduction rate after the first year of HFST application on ramps. For example, an untreated ramp in Milwaukee, Wisconsin, was the site of 87 crashes in one year. That ramp received HFST application in October 2011, and since then only two crashes have occurred on that ramp (Stoikes, 2014). Table 2.5 demonstrates hypothetical economic benefits and crash reductions after adopting HFST process (Mills, 2015). According to the statistics, if the site experienced an average of 1 crash per year prior to the application and that average was reduced

by 20% after application, HFST was a cost-effective solution for crash reduction. The Texas Transportation Institute utilized economic values of crash scenarios set by the FHWA to estimate the average cost of fatal and injury crashes to be \$158,177. HFST crash reduction effectiveness is shown in Figure 2.12.

**Table 2.5 Hypothetical scenarios of crash reductions and economic benefits (Mills, 2015)**

<b>Crash Frequency Before Treatment</b>	<b>Effective Crash Reduction, Economic Benefit</b>					
	<b>20% Reduction</b>		<b>30% Reduction</b>		<b>40% Reduction</b>	
	<b>1 Year</b>	<b>5 Year</b>	<b>1 Year</b>	<b>5 Year</b>	<b>1 Year</b>	<b>5 Year</b>
1	0.2	1	0.3	1.5	0.4	2
	31,635	\$158,177	\$47,453	\$237,266	\$63,271	\$316,354
3	0.6	3	0.9	4.5	1.2	6
	\$94,906	\$474,531	\$142,359	\$711,797	\$189,812	\$949,062
5	1	5	1.5	7.5	2	10
	\$158,177	\$790,885	\$237,266	\$1,186,328	\$316,354	\$1,581,770
7	1.4	7	2.1	10.5	2.8	14
	\$221,448	\$1,107,239	\$332,172	\$1,660,859	\$442,896	\$2,214,478



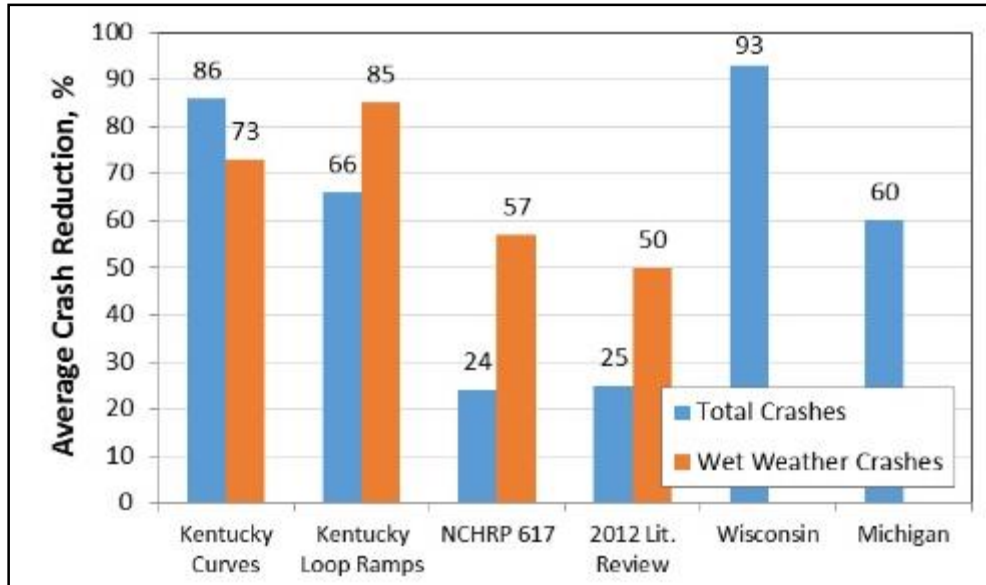


**Figure 2.12 HFST crash reduction effectiveness (Mills, 2015)**

HFST improves pavement friction without significantly affecting other surface qualities, such as noise, ride quality, or durability (Izeppi et al., 2010). Because most HFSTs are installed from point of curvature to point of tangent of a curve, the difference of noticeable sound level due to HFST is only a few seconds. Transtec Group, Inc. measured on-board sound intensity (OBSI) of HFST, determining that OBSI of HFST was 101.95 dBA when the OBSI of chip seal was 104.4 dBA.

HFST is a cost-effective solution compared to changing road geometric design, which requires extensive time and expense and can have environmental consequences. According to Baker (2013), HFST is the only safety solution that does not require driver response. Although the life expectancy of HFST depends on the type of roadway, geometric condition, traffic volume, and nature of traffic, international experience has indicated that proper installation of HFST can guarantee 7–12 years of service life. This study also reported more than 15 years of HFST service life applied on bridge decks. Similar to road surface performance, wear of high friction surfaces depends on construction quality, traffic demand, friction demand, climatic condition, and number

of heavy truck axles. Michigan DOT reported durability of HFST on bridge decks to be 12–15 years, including interstate highways with average daily traffic (ADT) of 48,000 to 62,000 vehicles per day (vpd).

Several studies were conducted independently to determine stopping distances on pavements treated with HFST. John LeFante from Interstate Road Management (IRM) reported that HFST successfully reduced stopping distances up to 40% when driving speeds were 60 mph (Figure 2.13), potentially reducing crash rates at intersections, rural roads, and pedestrian walkways.

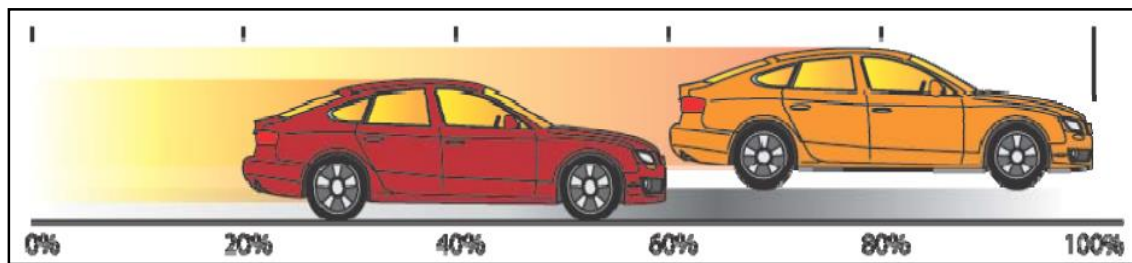


**Figure 2.13 Stopping distance reduction in HFST (LeFante, 2015)**

## **2.7 HFST Compared to Microsurfacing Treatment**

Microsurfacing utilizes asphalt emulsion and fine aggregates to mitigate raveling and oxidation of asphalt pavement surfaces (Figure 2.14). It also improves friction and appearance of concrete and asphalt surfaces (Peshkin et al., 2011). Microsurfacing is superior to HFST as a pavement preservation technique, but HFST provides more friction than microsurfacing. Microsurfacing extends the life of pavements, but HFST is not recommended for application on poor pavements. Microsurfacing generally provides good initial friction, but the friction deteriorates quickly, in some cases within two years of application (Michigan DOT). HFST improves friction number to more than 70 and sometimes up to 90, which is significantly higher than those as a result of microsurfacing (typically 40–50, sometimes up to 60).



**Figure 2.14 Typical Microsurfacing Treatment (Micro Surfacing, 2015)**

Typical pavement surface macrotexture depth is greater than 1.5 mm but in HFST, macrotexture depth ranges from 0.5 to 1.0 mm (Reddy et al., 2009). Pavements treated with microsurfacing have service life from 5 to 7 years, where HFST is an 8-12 year friction increasing method (Rajagopal, 2010). Wang et al. (2013) showed a benefit-cost ratio of microsurfacing from 1.42 to 4.13, but the FHWA has reported a cost-benefit ratio of more than 20 for HFST.

## **2.8 Causes of failure of HFST**

Factors such as raveling of material, delamination, and aggregate polishing can reduce the effectiveness of HFST (Izeppi et al., 2010). According to this study, improper mixing of the two parts of epoxy negatively affects epoxy performance. The two parts should be mixed according to the recommended ratio and for a certain period of time depending on the workplace temperature. In addition, creosol was previously used in most epoxy binders, but a strong odor and tendency to burn the skin during application lead to a decrease in creosol usage. Some studies found that

new epoxy formulations exhibit improper aggregate epoxy bonding than previous combinations that included creosol (Reddy et al., 2009).

Epoxy application rate should be consistently maintained and applied over the pavement surface, and aggregates should cover the wet binder completely; no binder should be visible once the aggregate is applied. Inadequate aggregate-epoxy placement can potentially cause treatment failure. Attention is required when applying HFST at night with poor visibility to ensure that the binder is adequately covered by the aggregate (Kelly, 2008). Uniform application of epoxy is difficult on porous or highly permeable surfaces, and incomplete application can also cause system failure. To ensure proper adhesion between the existing pavement and high friction aggregate, proper cleaning of the existing surface before HFST application is necessary.

Humidity and high moisture content can also hamper performance of epoxy over the pavement surface. At the time of HFST installation, the roadway must be dry and the temperature must be above the manufacturer's recommendation to avoid moisture trapped below the impermeable layer as the surface undergoes freeze-thaw action. This may lead to severe raveling and peel off of the high friction surface. Curing time and curing temperature are also significant factors in HFST failure. Pavements should not be open to the traffic before the required curing time, and recommended curing temperature should be maintained. If cured at a lower-than-recommended temperature, many epoxy resins do not reach fully designed strength, resulting in loss of aggregates and premature wear in wheel paths.

## **2.9 Unit Cost of HFST**

HFST installation costs depend on the type of project, labor cost, and cost of project components such as traffic control and treatment of pavement markings. Per unit treatment costs

previously ranged from \$30 to \$40/m<sup>2</sup>, but costs per m<sup>2</sup> are gradually decreasing for large projects and small bundled installations. Although, per unit cost of HFST is higher than other treatment processes, it provides increased safety and stability, and the life cycle cost is excellent, making HFST a good investment.

Total project cost, including cost for mobilization, traffic control, striping, remedial crack sealing, and sometimes patching, must be calculated in order to determine unit prices of HFST projects (Stoikes, 2014). According to this study, The Kentucky Transportation Cabinet had a significant number of HFST projects on two-lane roads with average project areas of 630 m<sup>2</sup>. HFST installation costs per project varied from \$14,000 to \$16,000 (unit cost \$20–\$30/m<sup>2</sup>). Stoikes reported another project that required a unit cost of \$20/m<sup>2</sup> with a total project area of 6,500 m<sup>2</sup>.

## **2.10 HFST projects in Kansas**

In 2009 the Kansas Department of Transportation (KDOT) contracted with the FHWA to do the High Friction Surface Materials Enhancing Safety at Horizontal Curves on the National System project (Meggers, 2015). Four locations were chosen to evaluate the long-term effectiveness and durability of high friction surface materials. The locations were K-99 in Wabaunsee County (two-lane asphalt pavement), K-5 in Leavenworth County (two-lane asphalt pavement), eastbound K-96/US-54 ramp in Wichita (concrete pavement) and northbound I-35/I-635 ramp in Kansas City (concrete pavement), as shown in Figure 2.15.

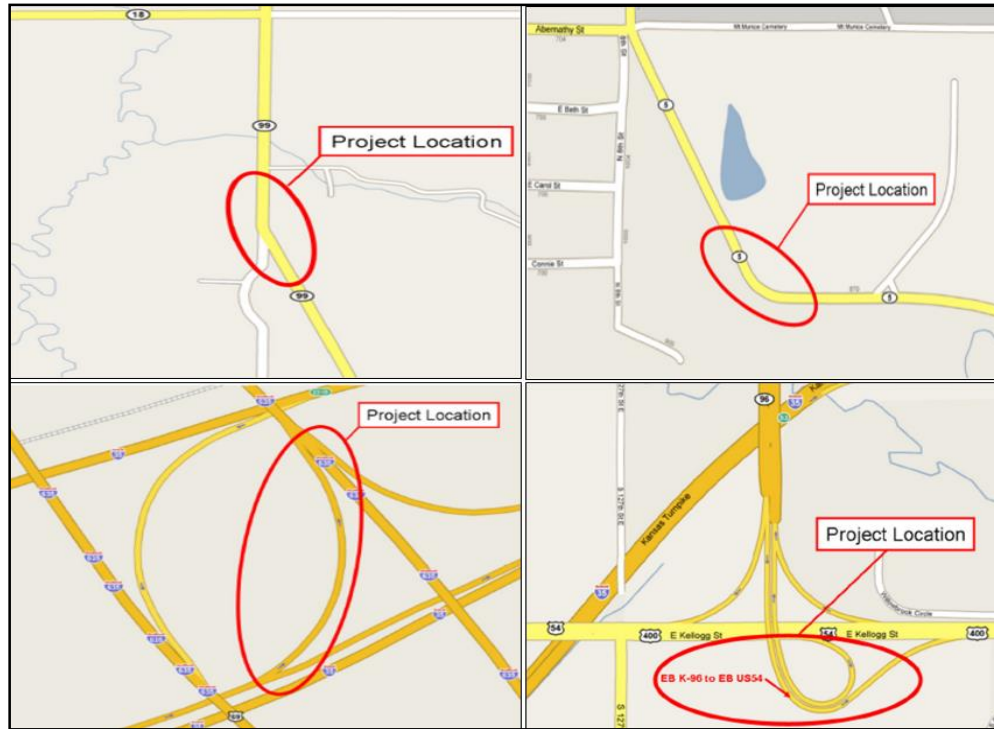


**Figure 2.15 HFST locations in Kansas: K-99, K-5, K-96/US-54, I-35/I-635 (clockwise from top left)**

All of four locations were treated with Poly Carb Type III epoxy-based overlay material and flint aggregate from Picher, Oklahoma. Pavement surface frictions were evaluated before treatment, immediately after treatment, and at later dates. Skid resistance testing was performed in addition to pull-off testing to determine bonding between HFST and existing pavement surface, and rapid chloride permeability (RCP) testing was performed to determine potential protection of underlying pavements from intrusion of moisture. According to specifications, asphalt surface cracks were filled with polymer and sand, and joints on the concrete surfaces were taped before applying high friction surfaces. KDOT determined epoxy application rate, which was initially 0.2 gal/m<sup>2</sup> but later increased to 0.27 gal/m<sup>2</sup>.

Skid values were evaluated before treatment, in late 2010, and in late 2013 (Meggers, 2015). Ribbed and smooth tire were used to determine skid number. Skid values improved

significantly after HFST application; smooth tire showed more improvement than ribbed tire. Rapid skid resistance losses were noticed on concrete surfaces. By 2013, decreasing skid values were nearly equal to initial skid values. Skid resistance on K-5 was better than other locations, but K-5 had the lowest traffic level of all testing sites. Pull-off test results exhibited significant asphalt bonding at the K-5 location. Complete failure of high friction surface bond to concrete substrate was observed on the I-35/I-635 and K-96/US-54 ramps. The K-99 location suffered from significant bond failure between 2010 and 2011 and was removed from the program. High friction surfacing on K-99 and K-5 locations are shown in figures 2.16 And 2.17.

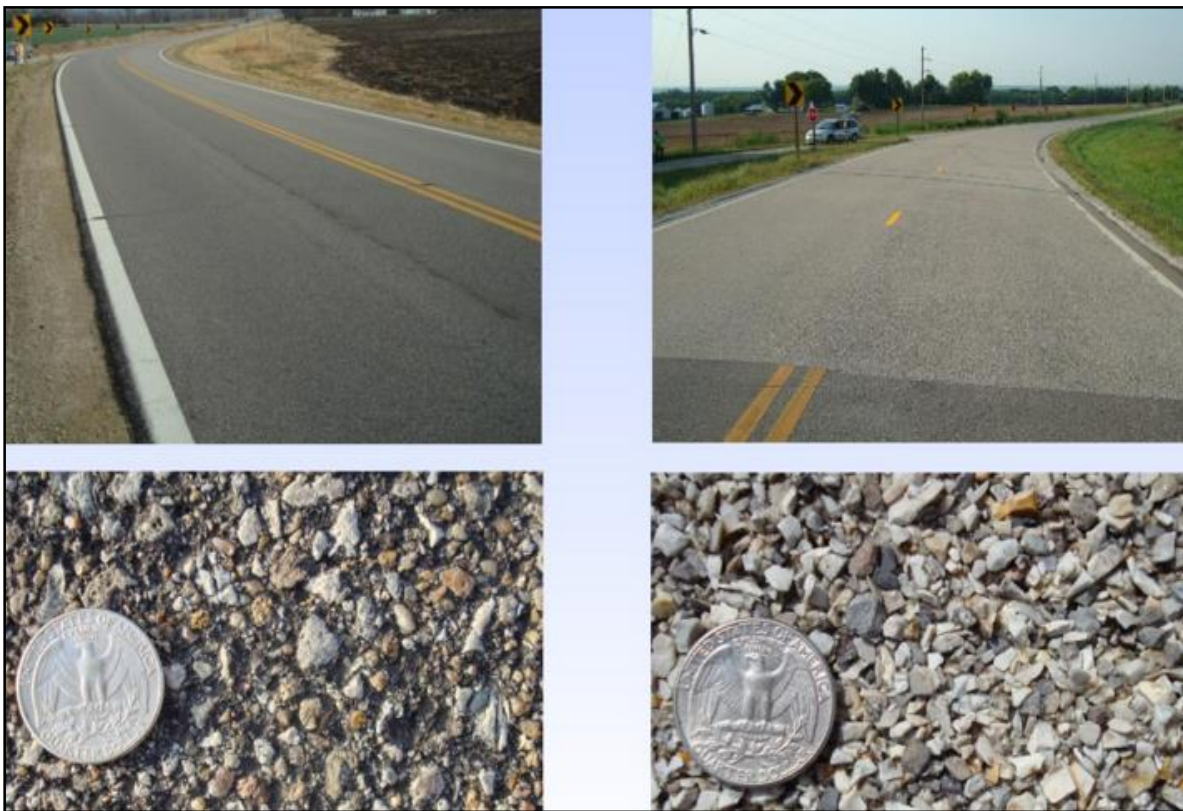


**Figure 2.16 Before and after HFST on K-99 in Wabaunsee County (asphalt pavement)**



**Figure 2.17 Before and after HFST on K-5 in Leavenworth County (asphalt pavement)**

Thicknesses of high friction surfaces in these projects were measured by removing cores from each location. Thickness was 3.05 mm on K-5 (asphalt), 3.25 mm on I-35/I-635 (concrete), and 3.85 mm for K-96/US-54 (concrete) application. The RCP test was also performed on the cores to determine permeability of the substrate paving material. RCP values indicated that the treatment afforded protection of the pavements from water penetration. K-5 had an RCP value of 33 coulombs on the top 50 mm and 167 on the bottom 50 mm of the core. Average RCP at the I-35/I-635 location was 856 coulombs on the top 50 mm and 1477 coulombs on the bottom 50 mm. At the K-96/US-54 location RCP was 1868 coulombs on the top 50 mm and 2983 coulombs on the bottom 50 mm. HFST projects on I-35/I-635 and K-96/US-54 locations were shown in figures 2.18 and 2.19.





**Figure 2.18 Before and after HFST on I-35/I-635 ramp in Kansas City (concrete pavement)**



**Figure 2.19 Before and after HFST on K-96/US-54 ramp in Wichita (concrete pavement)**

KDOT developed a specification for the material and placing of high friction surfaces in Kansas using the American Association of State Highway and Transportation Officials (AASHTO) provisional standard “High-Friction Surface Treatment for Asphalt and Concrete Pavements” (Meggers, 2015). KDOT implemented this specification on four HFST projects in 2014. Mill Valley Construction, Inc. applied HFST to southbound K-7 to K-32 exit ramp (Wyandotte County) in August 2014. After cleaning debris, epoxy binder was placed on a 150 ft. curved stretch, followed by application of the aggregate mix. HFST was applied in three other locations in Kansas in September 2014, as shown in Figure 2.20: southbound K-177/I-70 on ramp (Riley County), westbound I-70/K-177 off ramp (Riley County), and westbound K-18/I-70 on ramp (Riley County).



**Figure 2.20 HFST locations on K-177 (left) and K-18 (right)**

Bauxite aggregate was used for high friction surfacing in all three locations, and all locations contained both concrete and asphalt sections over which HFST was applied. In order to observe and compare differences in texture depth and friction characteristics before and after treatment, mean texture depths and skid values were collected using Laser Crack Measurement System (LCMS) and Locked Wheel Skid Trailer (LWST), respectively. After treatment the skid

number increased from 40 to 78; texture depth increased approximately 20% on asphalt sections and 55% on concrete sections (Zahir et al., 2015). Texture depth showed uniformity throughout the longitudinal pavement section with low standard deviation (less than 6%). However, the concrete section contained sharp increases and declines in texture depths, possibly due to the de-bonding of HFST at some locations (Figure 2.21), potentially resulting in varying texture depth values (standard deviation of 11%).



**Figure 2.21 De-bonding of high friction surface aggregates**

After treatment, skid number improved from 43 to 82 on the southbound K-177/I-70 on ramp. On the asphalt section, however, texture depths did not show consistent results, and in some spots values were even lower than initial values. Tests on these three locations were performed after one year of treatment, and within this time period de-bonding of high friction materials were observed in some spots, potentially causing inconsistent texture. The westbound I-70/K-177 off ramp exhibited significant texture depth improvement with consistent test results in asphalt and concrete sections. Texture depth increased approximately 12% and 57% on asphalt and concrete sections, respectively.

Texture depth and skid number of another roadway section on K-87 (Nemaha County) with chip seal surfacing was tested in order to compare to the friction or skid resistance of these three HFST locations. Texture depth and skid data before chip seal treatment were not available. The average skid number of this roadway section was 58, where the skid number of high friction surfaces varied from 71 to 82. In order to determine the friction number of these roadway sections, profile depth and coefficient of friction were calculated according to ASTM E-1960 specification using a Circular Track Meter (CTM) and Dynamic Friction Tester (DFT). Friction numbers of the chip seal-treated location varied from 46 to 50, but friction numbers on HFST locations varied from 50 to 58.

In 2016, KDOT is planning to apply HFST on K-7 and K-10 interchange loop ramp to provide additional friction between vehicle tires and ramp pavement. The interchange that will receive HFST is currently being reviewed based on crash data for each loop ramp. The interchange location is shown in Figure 2.22.

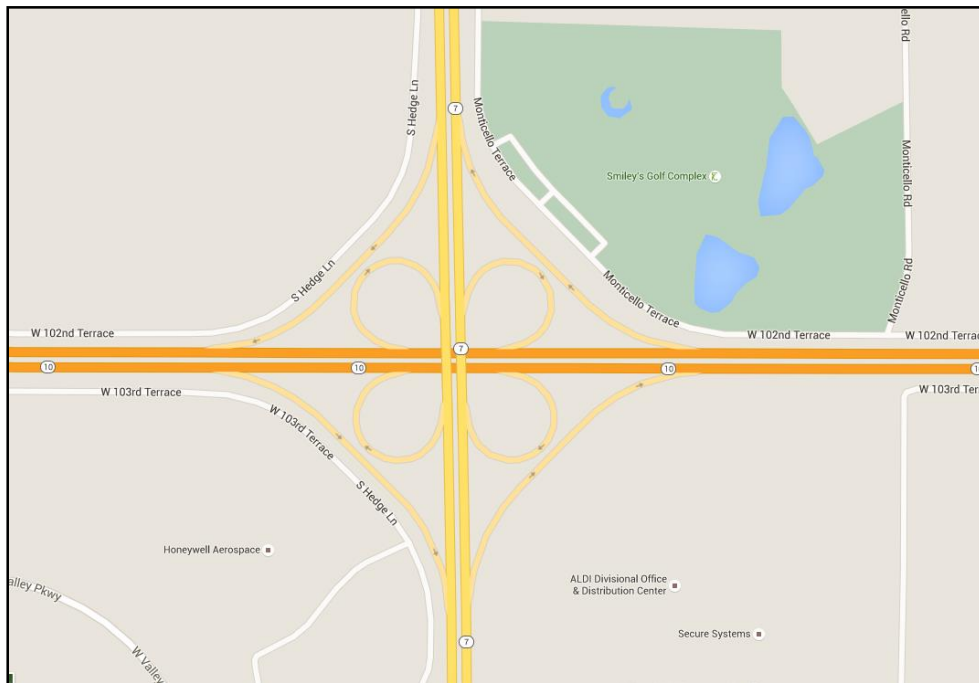


**Figure 2.22 K-7/K-10 interchange loop ramp**

## **2.11 Summary**

Approximately 10,000 fatal crashes occur each year on horizontal curves in the United States. Reduced friction between pavement and vehicle tires due to factors such as polishing of the aggregate in the pavement, wet weather, and speeding cause many of these lane or roadway departure crashes. Studies have found that more than 90% crashes were reduced after HFST, proving that HFST is the most effective method to address safety concerns at high friction demand locations. Other studies that recorded before-after crash data used cost-benefit analysis to justify use of HFST. Results of skid treatments applied by various state DOTs show that a 20% to 30% reduction in all crashes and a 50% reduction in wet weather crashes is a reasonable expectation for general HFST applications.

## **Chapter 3 - Methodology**

### **3.1 Field Tests**

In order to determine the performance of HFST, four KDOT highways were selected for investigation: K-18 westbound/I-70 westbound on-ramp (Riley County); K-177 southbound/I-70 westbound on-ramp (Riley County); I-70 westbound/K-177 northbound off-ramp (Riley County); and K-5 (Leavenworth County). First three locations contained both concrete and asphalt sections over which HFST was applied. The selected K-5 roadway section only had asphalt pavement over which HFS was applied. In order to observe and compare differences in texture depth and friction characteristics before and after treatment, mean texture depth and skid value were collected using Laser Crack Measurement System and Locked Wheel Skid Trailer, respectively.

#### **3.1.1 Laser Crack Measurement System**

The LCMS is composed of two high performance 3D laser profilers that measures complete transverse road profiles with 1-mm resolution at highway speed. The high resolution 2D and 3D data acquired by the LCMS is then processed using algorithms that were developed to automatically extract crack data including crack type (transverse, longitudinal, alligator) and severity, rutting (depth, type), potholes and raveling (Figure 3.1). LCMS can be operated under various types of lighting conditions and on various pavement types (Laurent et al., 2008). A data analyzing software analyzes data and reports MTD values of five standard AASHTO bands (center, right, and left wheel paths and outside bands).



**Figure 3.1** KDOT Laser Crack Measurement System used in this study

### **3.1.2 Locked Wheel Skid Trailer**

LWST, which measures steady-state friction force, contains a locked wheel that is dragged under constant load at a constant speed over wet pavement. Friction is determined from the resulting force and reported as skid number. High skid numbers represent greater skid resistance (Wambold, 1988). Two types of tire (ribbed and smooth) are used to measure skid numbers on roadway surfaces (Henry, 2000). The LWST can be operated near posted highway speed and can take measurements on longer stretch of roadway without causing lane closures (Figure 3.2).



**Figure 3.2** Locked Wheel Skid Trailer data collection

## 3.2 Laboratory Tests

### 3.2.1 Experimental Design

High friction surface treatment consists of two components: aggregate and binder. The aggregate should have a high polished stone value (PSV) and wearing resistance, and the polymer resin binder, unlike the asphalt-based binder, should be unaffected unless flooded with diesel fuel or solvents. Two aggregates, calcined bauxite and flint aggregate, and two epoxy binders, Mark-154 epoxy and Pro-Poxy Type III epoxy, were selected for this study, resulting in four epoxy-binder combinations:

Combination 1: Calcined bauxite aggregate and Mark-154 epoxy

Combination 2: Flint aggregate and Mark-154 epoxy

Combination 3: Calcined bauxite aggregate and Pro-Poxy Type III epoxy

Combination 4: Flint aggregate and Pro-Poxy Type III epoxy

### 3.2.2 Aggregate Tests

The GRIPGrain Chinese calcined bauxite (Figure 3.3) used in this project was a high density, high alumina, uniform-fired, manufactured product from Great Lakes Minerals (GLM). Tables 3.1 and 3.2 show the chemical composition and physical properties of the aggregate as provided by GLM.



**Figure 3.3 Chinese calcined bauxite aggregate used in this study**



**Table 3.1 Chemical composition of calcined bauxite aggregate (Great Lake Minerals)**

<b>Chemical Compound</b>	<b>Test Result</b>	<b>Specification</b>
Al <sub>2</sub> O <sub>3</sub>	88.10 %	87 % Min
Fe <sub>2</sub> O <sub>3</sub>	1.45 %	1.8 % Max
SiO <sub>2</sub>	5.10 %	7.0 % Max
TiO <sub>2</sub>	3.70 %	4.0 % Max
Na <sub>2</sub> + K <sub>2</sub> O	0.18 %	0.25 % Max
CaO + MgO	0.47 %	0.60 % Max

**Table 3.2 Physical properties of calcined bauxite aggregate (Great Lake Minerals, LLC.)**

<b>Test</b>	<b>Test Method</b>	<b>Result</b>
Bulk Density	(Not provided)	3.27 g/cc
Soundness	AASHTO T104	1.3
Polished Stone Value	AASHTO T279	71.0
Resistance to Degradation	AASHTO T96	9.3

The flint aggregate used in this project came from Picher, Oklahoma, and was supplied by Cornejo & Sons, a construction company from Wichita, Kansas (Figure 3.4). The supplier tested a few physical properties of the aggregate (dry and saturated surface dry specific gravity, moisture content, soundness ratio, compressive strength ratio, and percent wear) but did not test the chemical composition of the product. In this study, aggregate gradation, specific gravity, moisture content, and fine aggregate angularity tests were performed in the laboratory for both bauxite and flint aggregate in order to determine aggregate quality and compliance with specification. The supplier reported the flint aggregate's resistance to degradation as 9 (according to the AASHTO T96 test method), which indicates hard aggregate, but it contained significant amount of fine/dust particles. For that reason, Sand Equivalent (SE) and Durability Index (DI) tests were also performed for flint aggregate in addition to the four aggregate tests mentioned above.



**Figure 3.4 Pitcher, Oklahoma flint aggregate used in this study**

### **3.2.2.1 Aggregate gradation test**

Aggregate gradation test was performed according to Kansas test method KT-2, which reflects testing procedures in AASHTO T 27 and includes procedures for determining particle size distribution of aggregates using standard sieves. The set of sieves included 4.75 mm, 2.36 mm, 1.18 mm, 600  $\mu\text{m}$ , 300  $\mu\text{m}$ , 150  $\mu\text{m}$ , and 75  $\mu\text{m}$  sieve. Before testing, both aggregates were washed over a 75  $\mu\text{m}$  sieve to remove clay-like material since clay materials affect bonding between aggregate and binder. The aggregates were then dried in an oven with a uniform temperature of  $110 \pm 5$  °C for 24 hr. Aggregate gradation test was performed once the aggregates had cooled to room temperature.

Prior to the test, aggregate quartering was completed so that tests could be performed on a representative sample. For quartering, the aggregate was placed in the center of a clean surface and thoroughly mixed using a scoop; then a cone-shaped pile was formed. A large trowel was then vertically passed through the center of the pile to divide the sample in half. Each half was similarly divided into two parts, thereby quartering the sample. Opposite quarters were retained by rejecting

the other two quarters. The process was continued until the required sample size was obtained (Figure 3.5).

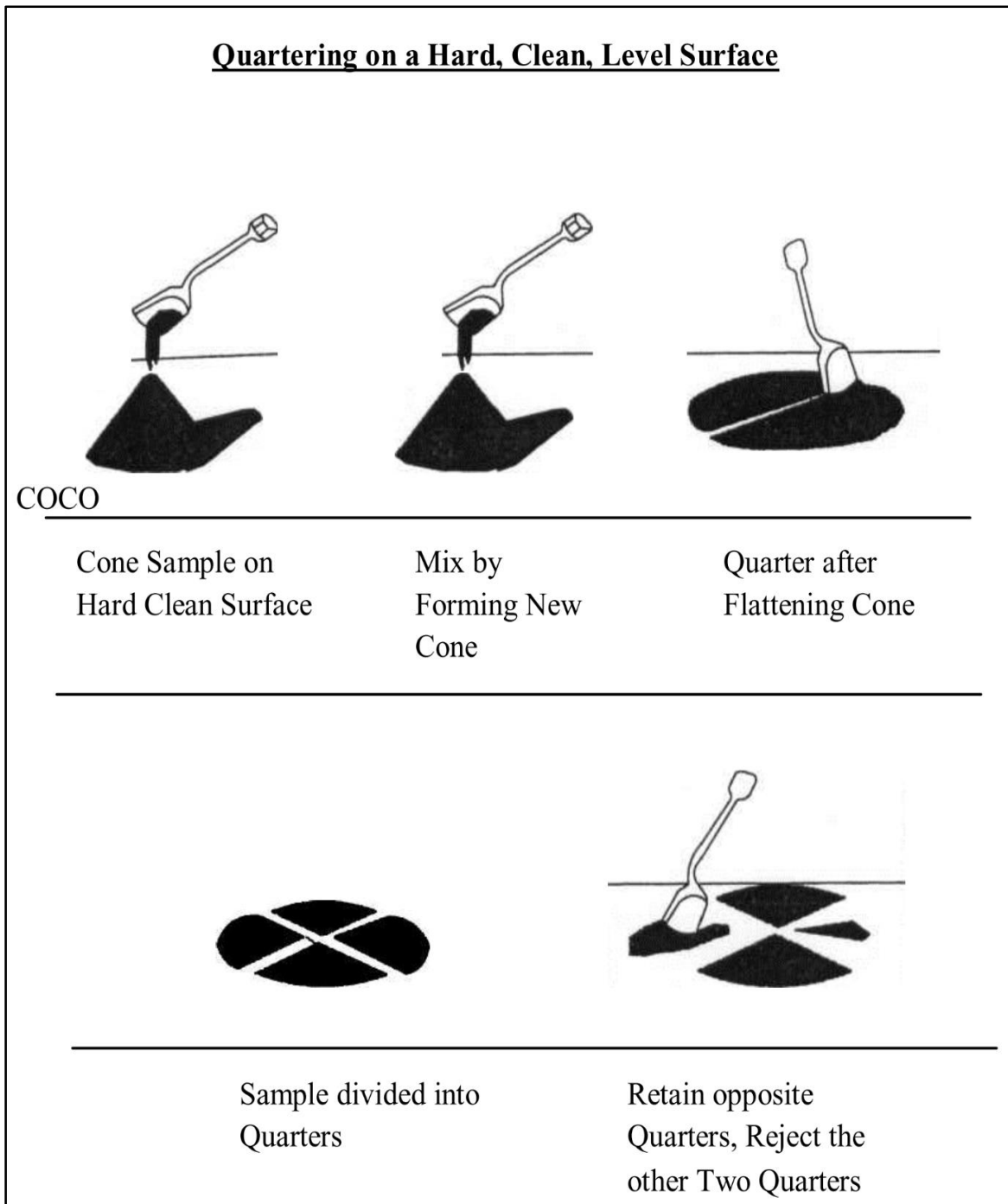


**Figure 3.5 Aggregate sample reduction using quartering method**

The washed, dried, and quartered aggregates were then weighed, and the dry mass was recorded. The sieves were then nested in decreasing order by placing sieves with small opening sizes below sieves with larger openings. One portion of the material was then poured on the top sieve, and then the sieves were covered and agitated by a mechanical sieve shaker. After shaking for 2 minutes, mass of the aggregate retained in each sieve was recorded. Total mass of material after sieving was expected to be within 0.3% of the total mass of the original dried sample. The total percentage of material retained on each sieve was calculated by

$$PR = \frac{100 (\text{Mass Retained})}{\text{Total Original Dry Mass of Sample}} \quad (3.1)$$

Where,

$PR$  = percentage of material retained on each sieve.

After calculating the percentage of material retained in each sieve, a gradation curve was drawn for both aggregates by placing sieve sizes (mm) along the x-axis and material retained percentage along the y-axis to determine particle size distribution.

### **3.2.2.2 Specific gravity test**

Specific gravity and absorption of both aggregates were determined according to Kansas test method KT-6, which reflects testing procedures in AASHTO T 84. According to the specification, this test was performed on the portion of aggregate that passed the 4.75 mm sieve and was retained on 150  $\mu\text{m}$  sieve. The required amount of aggregate was selected by quartering, and the selected portion was screened over the 4.75 mm sieve. All material retained on this sieve was discarded and then washed over the 150  $\mu\text{m}$  sieve to remove dust. The remaining aggregate portion was dried to a constant mass in the oven, and the dried mass of aggregate was recorded. The aggregate sample was then soaked in water for 24 hr and stirred vigorously. The aggregate was then removed from the water and brought to a saturated-surface dry condition by placing the

sample into a drying pan with a slightly rusty bottom and gently drying the sample using a manual dryer. The sample was stirred continuously to ensure uniform drying. The sample was frequently transferred from pan to pan until a saturated-surface dry condition was reached, as indicated by the absence of free moisture on the bottom of the pan. The weight of the aggregate was then recorded, which is the Saturated surface dry (SSD) weight. The saturate sample was then placed in a calibrated flask, and the flask was filled to the calibration mark with water that was  $25 \pm 1$  °C. The flask with its content was weighed, and then the aggregate was removed from the flask, dried to a constant mass in the oven, cooled at room temperature, and weighed. Specific gravity and absorption were calculated using the following formulas:

$$\text{Bulk specific gravity (dry)} = \frac{A}{C-W} \quad (3.2)$$

$$\text{Bulk specific gravity (SSD)} = \frac{B}{C-W} \quad (3.3)$$

$$\text{Absorption (\%)} = \frac{100(B-A)}{A} \quad (3.4)$$

Where,

$A$  = mass of oven-dried sample in air (gm)

$B$  = mass of SSD sample in air (gm)

$C$  = mass of water to the calibration line

$W$  = mass of water added to the flask (gm).

### **3.2.2.3 Moisture content test**

Moisture content test was performed according to Kansas test method KT-11, which reflects testing procedures in AASHTO T 265. Moist and clean flint aggregate is shown in figure 3.6. For this test, a clean, dry container was weighed, and a representative moist sample after quartering was placed into that container. The container was then weighed, and the mass was recorded. The container with moist sample was then placed into the drying oven with a maintained

temperature of  $110 \pm 5$  °C and dried at a constant mass. The sample was initially dried overnight (16 hr), and the mass was recorded; then the sample was dried again for 4 hr and weighed. The sample weight was identical in both instances; no change in mass in two successive drying periods indicated that the sample dried completely. Moisture content of both aggregates was calculated using Equation 3.5 or 3.6.

$$W = \left[ \frac{\text{mass of moisture}}{\text{mass of oven dried sample}} \right] \times 100 \quad (3.5)$$

Or,

$$W = \left[ \frac{(W_1 - W_2)}{(W_2 - W_c)} \right] \times 100 \quad (3.6)$$

Where,

$W$  = moisture content (%)

$W_1$  = mass of container and moist sample (gm)

$W_2$  = mass of container and oven-dried sample (gm)

$W_c$  = mass of container (gm).



**Figure 3.6 Moist flint (left) and clean flint (right) aggregate**

### 3.2.2.4 Fine aggregate angularity test

Fine aggregate angularity (FAA), or aggregate uncompacted void content test was performed according to Kansas test method KT-50, which reflects testing procedures in AASHTO T 304. For this test, aggregate sample was washed over a 75  $\mu\text{m}$  sieve and dried completely. Dried aggregate was then sieved over 2.36 mm, 1.18 mm, 600  $\mu\text{m}$ , 300  $\mu\text{m}$ , and 150  $\mu\text{m}$  sieves. A total of 190 gm of sieved material was tested in the following combinations:

2.36 mm to 1.18 mm	44 gm
1.18 mm to 600 $\mu\text{m}$	57 gm
600 $\mu\text{m}$ to 300 $\mu\text{m}$	72 gm
300 $\mu\text{m}$ to 150 $\mu\text{m}$	17 gm

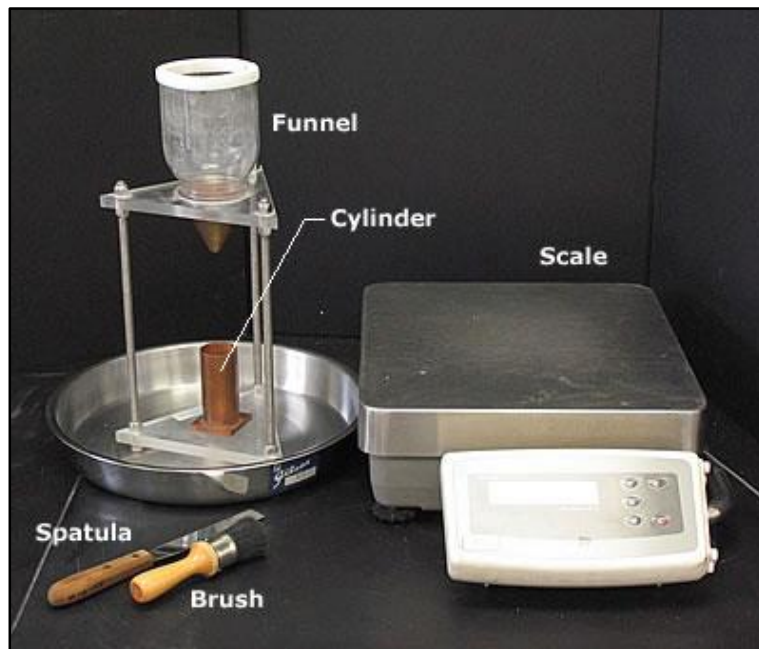


**Figure 3.7 Experimental setup of fine aggregate angularity test**

Prepared sample was then mixed homogeneously. Figure 3.7 shows the experimental setup of this test. The funnel opening was blocked with one finger, and the sample was poured into the funnel. The sample was then allowed to fall freely into the measure, and excess heaped aggregate

from the measure was removed by a single pass of a spatula. Content of the cylinder was then poured into a 200 mL volumetric flask, and the content was weighed and recorded. Distilled water at  $25 \pm 1$  °C was poured into the flask to the calibration mark. The cylinder with the aggregate and water is weighed, and weight was recorded. Uncompacted void content ( $U_k$ ) was calculated by following equations:

$$U_k = \frac{U_1 + U_2}{2} \quad (3.7)$$

$$U_{1, 2} = \frac{100 [V_w - (V_f - V_c)]}{V_c} \quad (3.8)$$

Where,

$U_1$  and  $U_2$  = uncompacted void contents of Trial No. 1 and Trial No. 2, respectively

$V_w$  = volume of water (mL)

$V_f$  = volume of flask (mL)

$V_c$  = calibrated volume of cylinder (mL).

### 3.2.2.5 Sand equivalent test

Sand equivalent test was performed according to American Standard of Testing Materials (ASTM) D 2419 specifications, which reflect testing procedures in AASHTO T 176. Fine aggregates often contain desirable coarse particles, sand-sized particles, and generally undesirable clay or plastic fines and dust. Because flint aggregate from Picher, Oklahoma, contains more fine particles than calcined bauxite, the sand equivalent test was performed only for the flint aggregate. Under standard conditions this test indicates relative proportions of clay-sized or plastic fines and dust in fine aggregates that pass the 4.75 mm sieve. Desirable amount of aggregate passing 4.75 mm sieve was taken, and necessary moisture conditions were ensured for the aggregate. A siphon assembly (Figure 3.8) was fitted to a 1.0 gallon (3.8 L) bottle of calcium chloride solution, and the bottle was placed on a shelf  $90 \pm 5$  cm above the working surface. A total of  $102 \pm 3$  mm of



working calcium chloride solution was siphoned into a plastic cylinder. The aggregate sample was then poured into the cylinder using a funnel to avoid spillage. The wetted specimen was allowed to stand undisturbed for  $10 \pm 1$  minutes. At the end of the 10-minute soaking period, the cylinder stopper was attached to it, and the cylinder was placed into a mechanical sand equivalent shaker that shook the cylinder and its contents for  $45 \pm 1$  seconds.

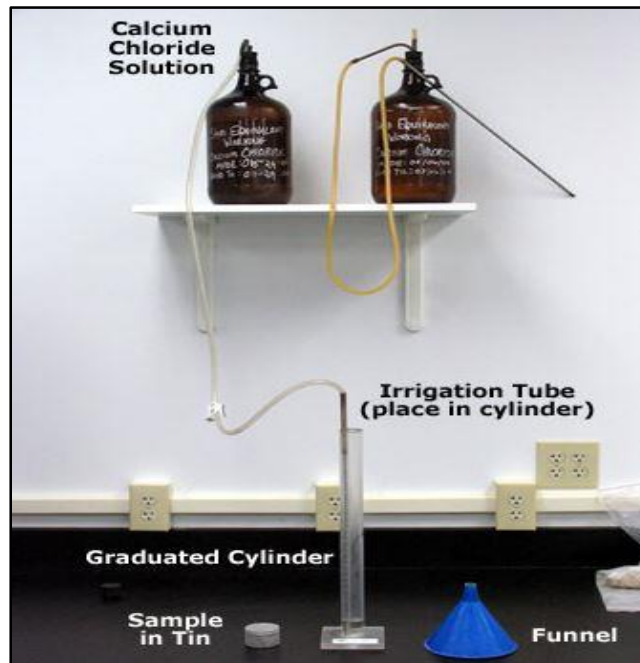


**Figure 3.8 Siphon assembly with irrigator tube**

Following the shaking operation, the cylinder was set upright on the working table, and the stopper was removed. An irrigation tube was then inserted into the cylinder, gently stabbed, and twisted. The irrigation tube was then removed, and the cylinder and content remained undisturbed for  $20 \text{ minutes} \pm 15 \text{ seconds}$ . Following the 20-minute rest period, the level of the top of suspension was recorded, a measurement referred to as the clay reading. Sand and clay readings are shown in figure 3.9 below. The weighted foot assembly was then placed over the cylinder and lowered until it rested on the sand. A total of 25.4 cm was subtracted from the level indicated by the extreme top

edge of the indicator, a value known as the sand reading. Sand equivalent was calculated by equation 3.9.

$$SE = \left( \frac{\text{sand reading}}{\text{clay reading}} \right) \times 100 \quad (3.9)$$

Where,

$SE$  = sand equivalent of the sample

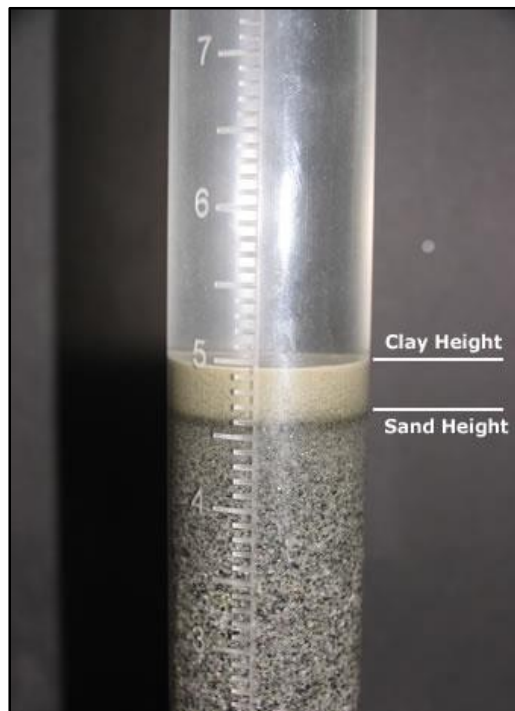


**Figure 3.9 Sand and clay reading in sand equivalent test**

### **3.2.2.6 Aggregate durability index test**

Durability index of aggregates was determined according to AASHTO D 3744 specifications. Calculated durability index value indicates the relative resistance of an aggregate to produce detrimental clay-like fines when subjected to prescribed mechanical methods of degradation. Similar to the sand equivalent test, durability index test was performed only for the flint aggregate; however, this test utilized a shaking time of 10 minutes instead of 45 seconds. Durability index value of fine aggregate was determined by the following equation:

$$DI = \left( \frac{\text{sand reading}}{\text{clay reading}} \right) \times 100 \quad (3.10)$$

Where,

$DI$  = durability index of the sample

### 3.2.3 Preparation of Slab Specimen

In this study slabs were compacted in a kneading slab compactor in the laboratory. Prepared slabs will simulate the existing roadway surfaces. A commercial 'grade A' Superpave mix known as SM 12.5A was used for compacting slabs. The dimensions of each slab were 32cm×26cm×4.5cm (12.75in.×10.25in.×1.8in.). Before compacting, the superpave mixture experienced short-term aging when it was placed in an oven at 150 °C for 2 hr according to Kansas standard test method KT-58. The slab was then compacted in the compactor to achieve  $8 \pm 1\%$  air voids. A picture of the compacted slab is shown in Figure 3.10. Compacted slab specimens simulated existing asphalt surfaces on which HFST was applied in the laboratory. In order to simulate field aging, slabs were cooled for 16 hr before they were removed from the mold. Theoretical maximum specific gravity ( $G_{mm}$ ) of the loose mixture was determined to be 2.390 according to Kansas test method KT-39. By using equation 3.11, mass of each slab sample was determined for 8% air voids:

$$\begin{aligned} \text{Mass of each sample} &= \frac{(1-0.08) \times 2.390 \times 12.75 \times 10.25 \times 1.8 \times 1000}{12^3 \times 3.2808^3} & (3.11) \\ &= 8.476 \text{ kg} \end{aligned}$$



**Figure 3.10 Compacted slab in kneading slab compactor**

### **3.2.4 Epoxy Application**

Two epoxy resins, Polycarb Mark-154 and Pro-Poxy Type III epoxy, were used in this study. Both epoxies consisted of parts A and B, and a unique Jiffy mixer (Figure 3.11) was used to mix equal volumes of both parts for 3-4 minutes (Figure 3.12).



**Figure 3.11 Jiffy mixer used for epoxy mixing**



**Figure 3.12 Mixing of part A and B of the epoxy**

Because both epoxies were thermosetting, aggregates had to be broadcast in a timely manner over the epoxy. An initial curing time was required after applying the epoxy and aggregate over the slabs, and the curing time in the laboratory, based primarily on temperature, was 4 hours. Properties of both epoxies are listed in Table 3.3.

**Table 3.3 Material properties of the epoxy used**

<b>Property</b>	<b>Polycarb Mark-154</b>	<b>Pro-Poxy Type III</b>
Viscosity	1000 cP	1500 Cp
Gel Time	20 minutes (@ 25 °C)	20 minutes (@ 25 °C)
Compressive Strength	8500 psi	>5000 psi
Tensile Strength	2500 psi	>3000 psi
Elongation	45 to 55%	>30%

### **3.2.5 High Friction Surface Preparation**

For preparing high friction surfaces, slab surfaces in this study were broom cleaned since clean, dry surfaces are required for HFST application. In addition, duct tape was applied on four

vertical sides of the slab (Figure 3.13) to prevent loss of epoxy and aggregate through the sides of the slabs. According to the KDOT-specified epoxy application rate of 1 gal over 1.85-2.8 m<sup>2</sup>, 134 ml Polycarb Mark-154 epoxy was used to cover the surface of one slab (32 cm ×26 cm). Although this epoxy application rate was sufficient for the flint aggregate, this rate of application did not allow proper bonding for the bauxite aggregate; therefore, the epoxy application rate was increased to 0.4 gal/yd<sup>2</sup> for bauxite aggregate. The rate for flint aggregate was 0.35 gal/yd<sup>2</sup>.



**Figure 3.13 Duct tape applied on sides of the slab to prevent epoxy loss**

Aggregates were broadcast within a few minutes of applying the epoxy. Step by step epoxy and aggregate application process is shown from figure 3.14 to figure 3.16. In order to cover each slab, 850 gm of aggregate was broadcast evenly over the epoxy layer. After 4 hr of curing, a soft brush was used to gently sweep excess aggregates. The amount of loose flint aggregates from one slab was 400 gm and 250 gm for loose bauxite aggregates. Subsequent aggregate application rates for both aggregates were calculated as 6 kg/yd<sup>2</sup> for bauxite aggregate and 4.5 lb/yd<sup>2</sup> for flint aggregate.

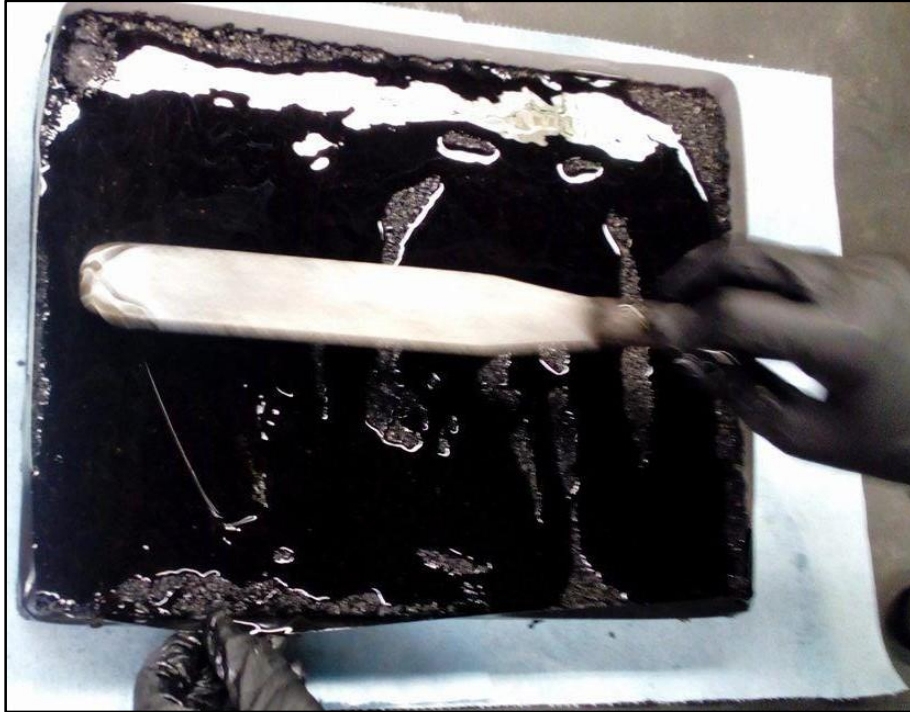


**Figure 3.14 Epoxy application over the slab**



**Figure 3.15 Slab covered with epoxy**



**Figure 3.16 Aggregate is being spread over the epoxy covered slab**

### **3.2.6 Tests performed on Prepared High Friction Surfaces**

After preparing the high-friction surfaces in the laboratory, circular track meter and dynamic friction tester readings were taken on bare slabs before and after HFST application in order to evaluate friction improvement as a result of the treatment. Slabs with HFST were then tested in a Hamburg Wheel Tracking Device for 2,000 wheel-load repetitions to simulate field traffic. The objective of this test was to observe whether there is any de-bonding of the aggregates from the slab after 2,000 wheel passes. Upon completion of the test, slabs were allowed to dry completely and tested again with CTM to assess texture depth characteristics.

#### **3.2.6.1 Testing with a circular track meter**

A CTM was used to obtain and analyze pavement macrotexture profiles according to the ASTM E 2157 standard test method. A CTM contains a charge-coupled device (CCD) laser displacement sensor mounted on an arm that rotates along a circular track with a diameter of 284 mm and a circumference of 892 mm. A CTM divides the track circumference into eight segments, measures the texture depth of all the segments, and then calculates the average, or mean profile



depth (MPD). CTM can be used for laboratory investigations or paved surfaces in the field (Figure 3.17). The device is controlled by a computer that saves and processes the data. When measurement is initiated by the computer, a DC (direct current) motor drives the arm for a full 360° revolution. Computer software developed for the CTM reports MPD and root mean square (RMS) values of the macrotexture profiles.



**Figure 3.17 Circular track meter for measuring texture depth**

In this study, the CTM was tested before each measurement using the verification panel provided by the manufacturer. For texture depth measurement, the slabs were cleaned before testing, the CTM was placed over the slab, options were set from the computer to compute the surface MPD, and the data were recorded.

### 3.2.6.2 Testing with a dynamic friction tester

A DFT was used to measure paved surface frictional properties as a function of speed. Tests were performed in the laboratory according to the ASTM E 1911 standard test method. A DFT contains a horizontal spinning disk in the bottom fitted with three spring-loaded rubber sliders (Figure 3.18) that contact the paved surface as the disk rotational speed decreases due to friction generated between the sliders and the paved surface. A water supply unit delivers water to the paved surface being tested, and torque is monitored continuously as the machine begins operation. Velocity decreases due to friction between the sliders and the test surface. Friction at 20, 40, 60, and 80 km/hr were recorded, and the frictional coefficient was determined (Figure 3.19). Similar to CTM, this device is controlled by a computer that saves and processes the data. The DFT can be used for laboratory investigations and on paved surfaces in the field.

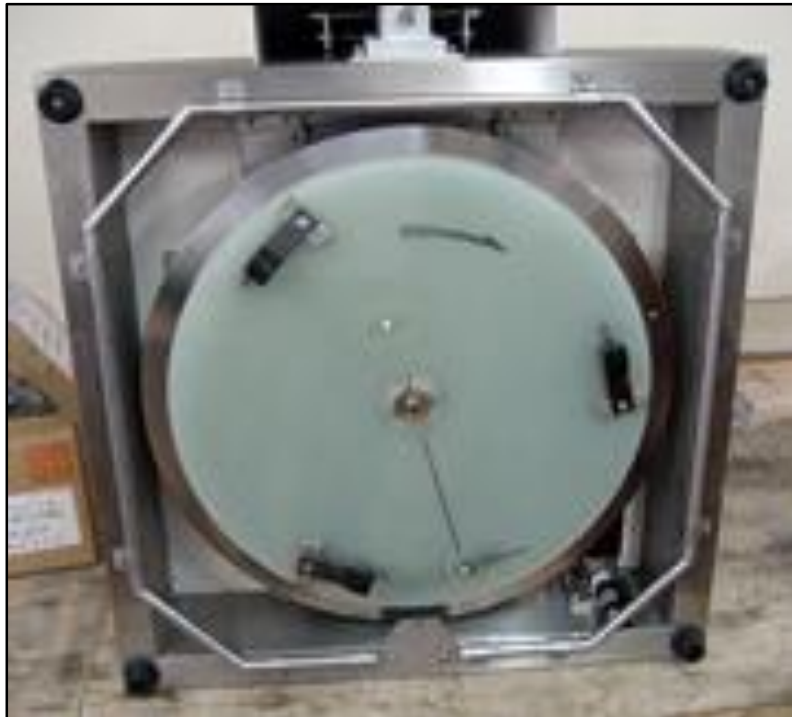


**Figure 3.18 Rubber sliders fitted in the bottom of DFT**

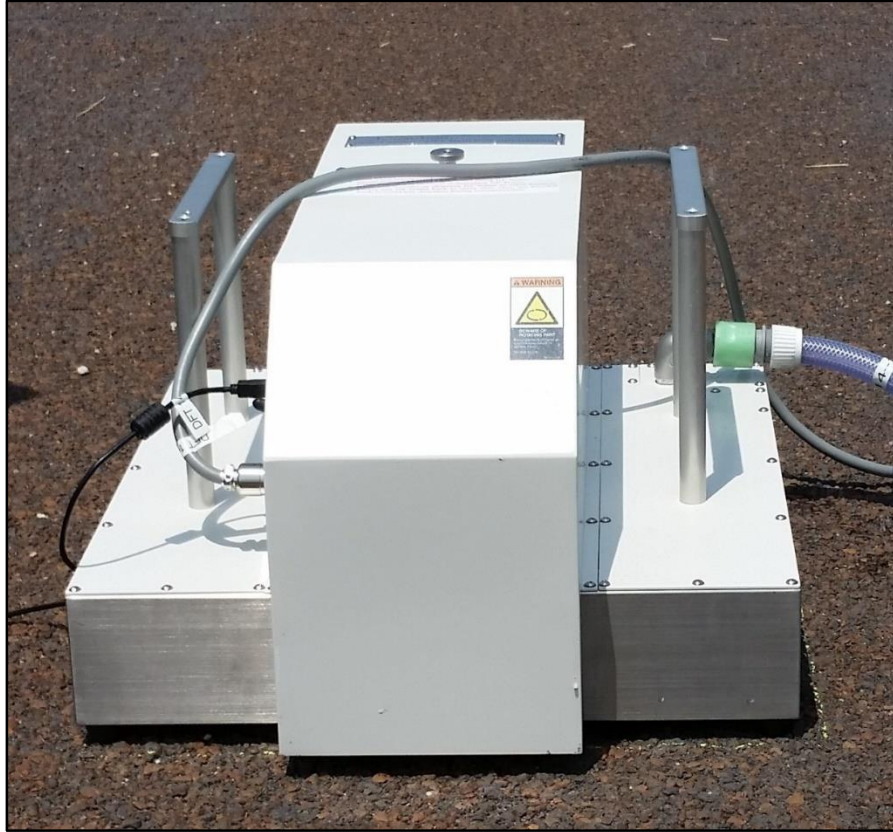


**Figure 3.19 Dynamic friction tester for measuring frictional coefficient**

The friction number (FN) of a surface can be calculated from CTM and DFT readings. In order to calculate the FN in this study, the DFT was placed over the same area where CTM readings were taken. According to ASTM E 1960 specifications, FNs were calculated from the following formula:

$$FN = 0.081 + 0.732 (DFT_{20}) e^{\left(\frac{-40}{S_p}\right)} \quad (3.12)$$

$$S_p = 14.2 + 89.7 (MPD) \quad (3.13)$$

Where,

$FN$  = friction number of the surface

$DFT_{20}$  = DFT frictional coefficient at 20 km/hr and

$MPD$  = corresponding CTM reading.

### 3.2.6.3 Testing with a Hamburg Wheel Tracking Device

According to AASHTO T 324 standard test procedure, an HWTD test was performed in which two loaded wheels, each weighing 72 kg were run over the prepared HMA specimens (figure 3.20). Rut depths were evaluated to determine the wearing resistance and bonding of HFSs under repeated wheel load. The tests were performed by submerging the slab specimens under water at 50 °C, and rut depth was measured after 2,000 wheel passes. CTM readings were taken before and after the HFST application; the data were then compared to ensure that bonding between aggregate and epoxy was satisfactory.

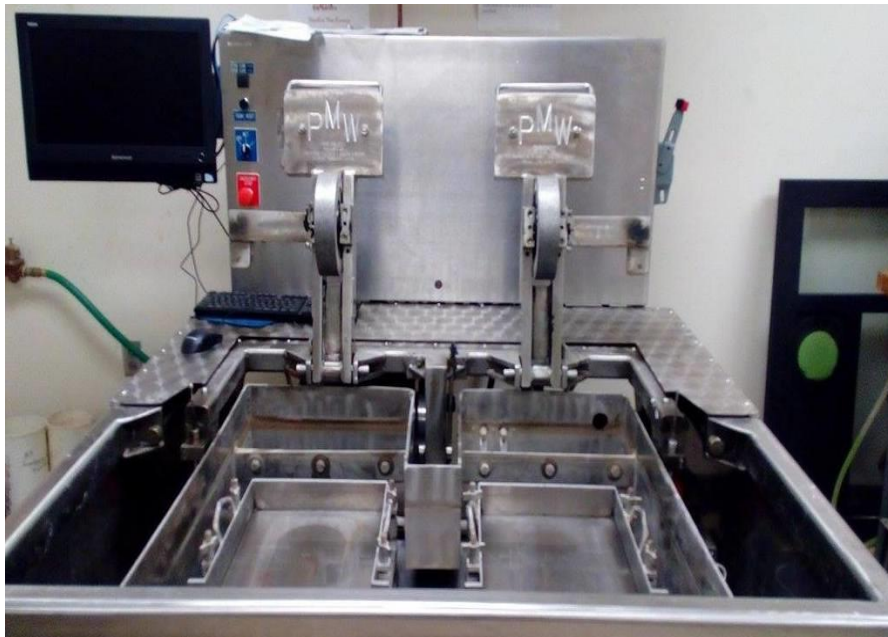


**Figure 3.20 Hamburg Wheel Tracking Device**

# Chapter 4 - Results and Discussion

## 4.1 Field Test Results

### 4.1.1 K-18 westbound and I-70 westbound on-ramp

In September 2014, HFST was applied on the roadway section of westbound K-18 and the on-ramp for westbound I-70. This roadway contained asphalt and concrete pavement sections with applied HFST. LCMS texture depth readings and LWST skid data were collected before and after placement of HFST in order to observe and compare differences in texture depth and friction characteristics before and after treatment. Before treatment, mean texture depth of this roadway section was 0.8 mm with a standard deviation of 0.053 mm and a coefficient of variation of 6.7%. After high friction surface treatment, texture depth increased to 1.02 mm with a standard deviation of 0.051 and a coefficient of variation of 5.0% (Figure 4.1). Skid numbers were evaluated using smooth and grooved tires both before and after treatment.

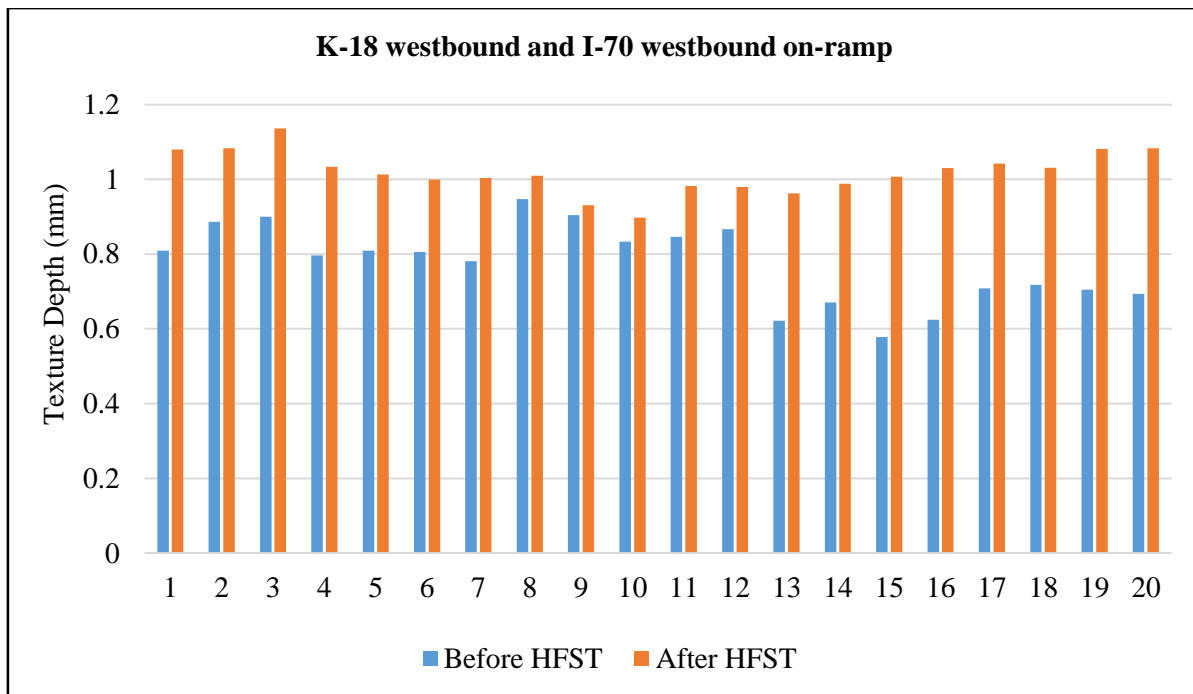


Figure 4.1 Texture depth values along K-18/I-70 on-ramp

### 4.1.2 K-177 southbound and I-70 westbound on-ramp

This roadway section also had asphalt and concrete sections with high friction surface applied over it in September 2014. LCMS texture depth and LWST skid data were collected before and after treatment. Grooved and smooth tires were used for skid number measurements. Before high friction surface treatment, mean texture depth of this roadway section was 0.94 mm with a standard deviation of 0.092 mm and a coefficient of variation of 6.1%. After high friction surface treatment, texture depth increased to 0.94 mm with a standard deviation of 0.061 mm and a coefficient of variation of 4.6% (Figure 4.2).

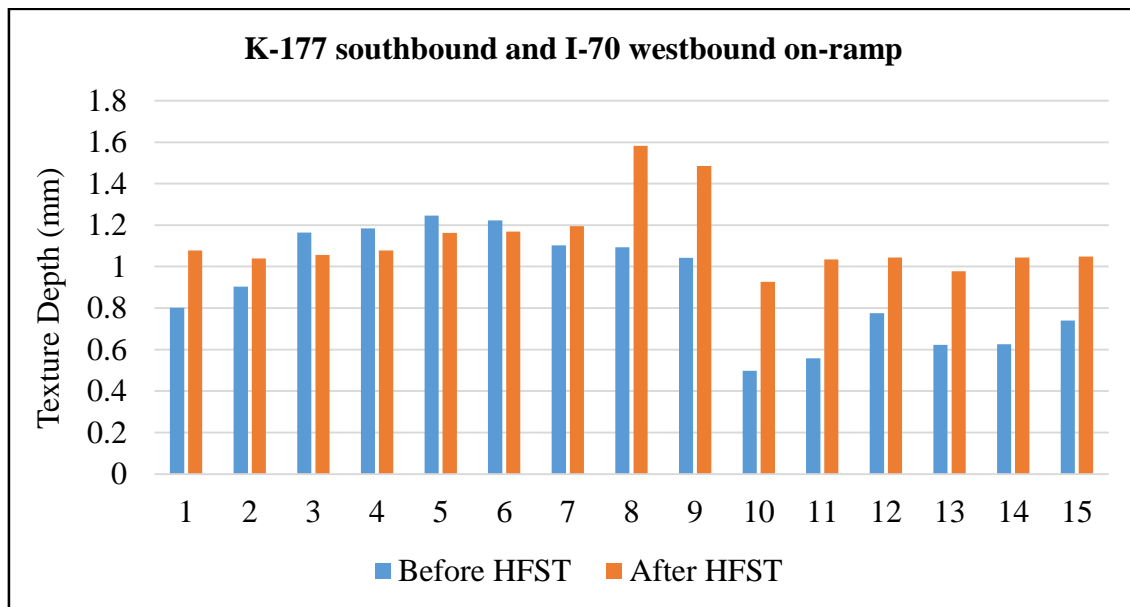
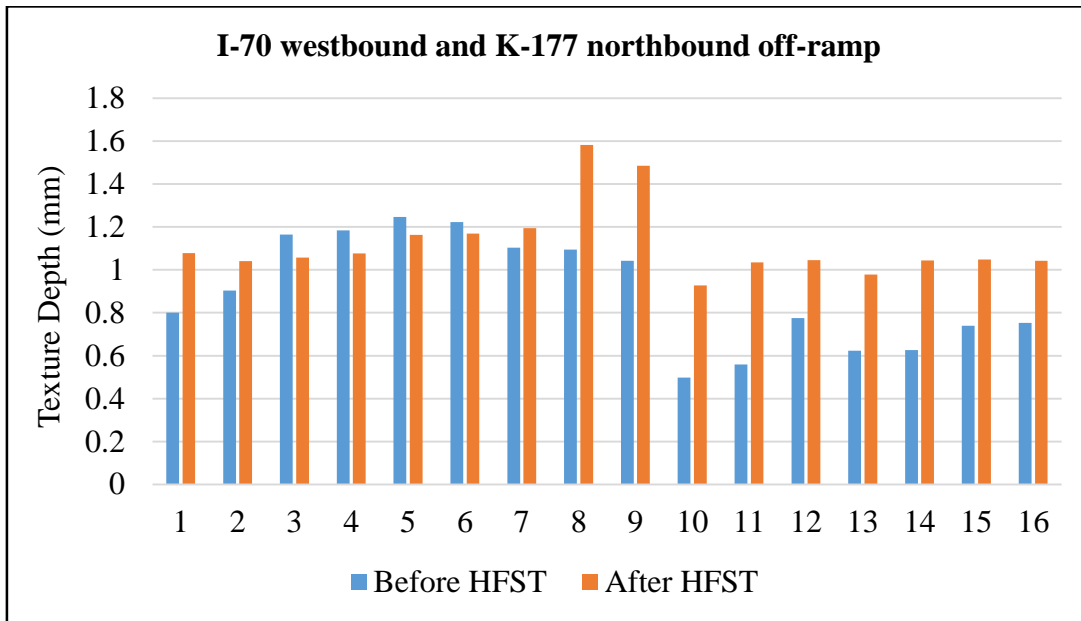


Figure 4.2 Texture depth values along K-177/I-70 on-ramp

### 4.1.3 I-70 westbound and K-177 northbound off-ramp

The roadway sections of the I-70 off-ramp and northbound K-177 also contained asphalt and concrete pavement sections with HFST. Before high friction surface treatment, mean texture depth of this roadway section was 0.86 mm with a standard deviation of 0.11 mm and a coefficient of variation of 10%. After high friction surface treatment, texture depth increased to 0.12 mm with a standard deviation of 0.071 mm and a coefficient of variation of 4.2% (Figure 4.3). At some

locations, ‘after HFST texture depth’ readings were less than ‘before HFST readings’. However, data on this section were collected approximately one year after HFST placement instead of immediately after treatment, so de-bonding of HFST at some spot occurred which could be a reason for that (figure 4.4).



**Figure 4.3 Texture depth values along I-70/K-177 off-ramp**



**Figure 4.4 De-bonding of high friction surfaces**

#### 4.1.4 K-5 roadway with high friction surface

High friction surface was applied on the K-5 roadway section in August 2009. Texture depth and skid data were collected after the treatment. LWST and LCMS before the treatment were not available, so comparison of texture depth and skid number could not possible for this roadway section. Mean texture depth after treatment was 0.87 mm with a standard deviation of 0.022 mm and a coefficient of variation of 2.49 mm. Skid data were collected using both grooved and smooth tires.

#### 4.1.5 Relationship between Texture depth and Skid number

In order to compare Skid Number (SN) with mean texture depth (MTD), MTD values on all locations on asphalt and concrete pavement were averaged. Average LWST skid number values pertained to the entire roadway section with both types of pavement. Average MTD values were plotted against skid number values to determine the possible correlation between skid and texture depth. Figure 4.5 and 4.6 shows that a good correlation was found between MTD and SN for roadways with high friction surfaces using grooved and smooth tires.

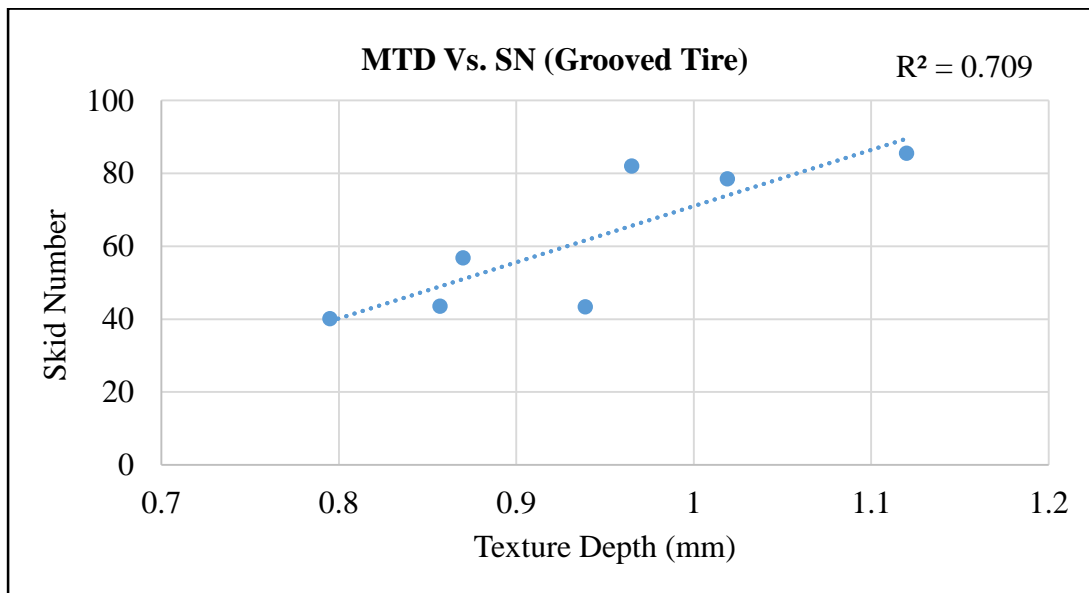


**Figure 4.5 Relationship between texture depth and skid (using Grooved tire)**



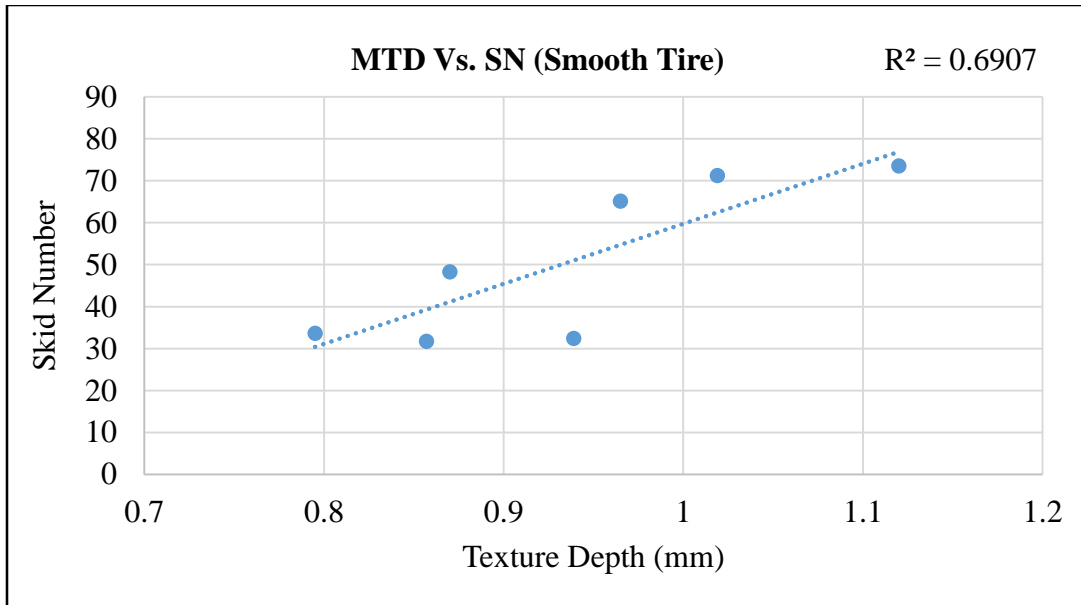


**Figure 4.6 Relationship between texture depth and skid (using Smooth tire)**

## **4.2 Laboratory Test Results**

### **4.2.1 Aggregate test results**

#### **4.2.1.1 Aggregate gradation test result**

An aggregate gradation test was performed according to Kansas test method KT-2 in order to determine particle size distribution of bauxite and flint aggregates. Table 4.1 and 4.2 tabulates results of the gradation test.

**Table 4.1 Aggregate gradation test results of bauxite aggregate**

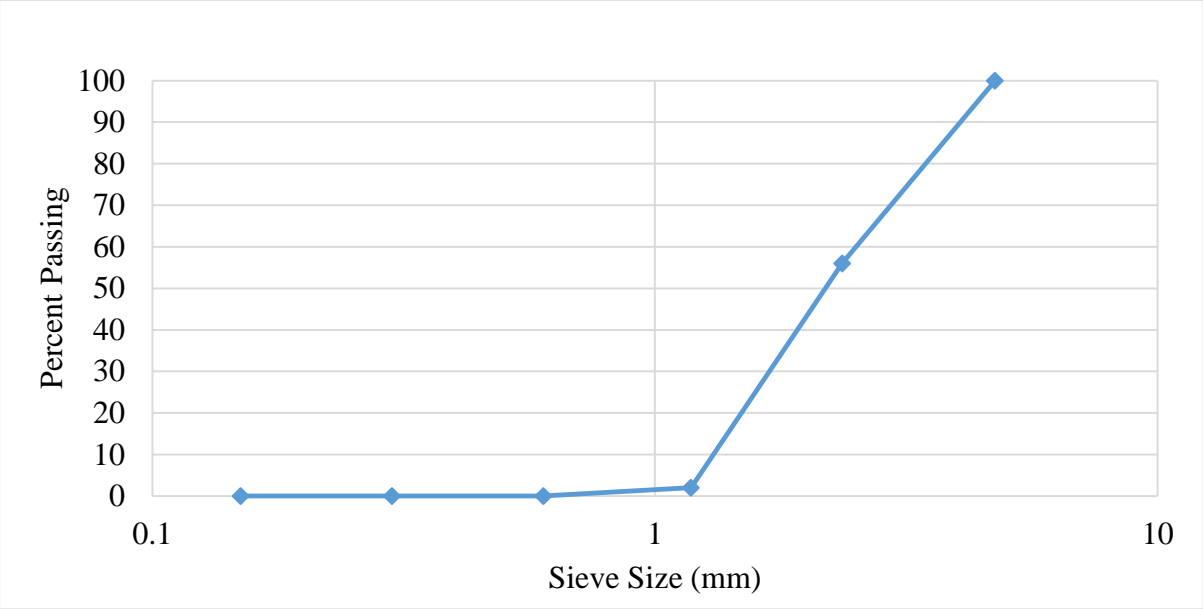
<b>Sieve No.</b>	<b>Sieve Size</b>	<b>Retained (gm)</b>	<b>Percent Retained</b>	<b>Cumulative Percent Retained</b>	<b>Percent Finer</b>
4	4.75	0.1	0	0	100
8	2.36	727.1	44	44	56
16	1.18	900.7	54	98	2
30	0.6	34.3	2	100	0
50	0.3	0.7	0	100	0
100	0.15	0.4	0	100	0
200	0.075		0	100	0
Pan	<0.0625	1.1	0	100	0

**Table 4.2 Aggregate gradation test results of bauxite aggregate**

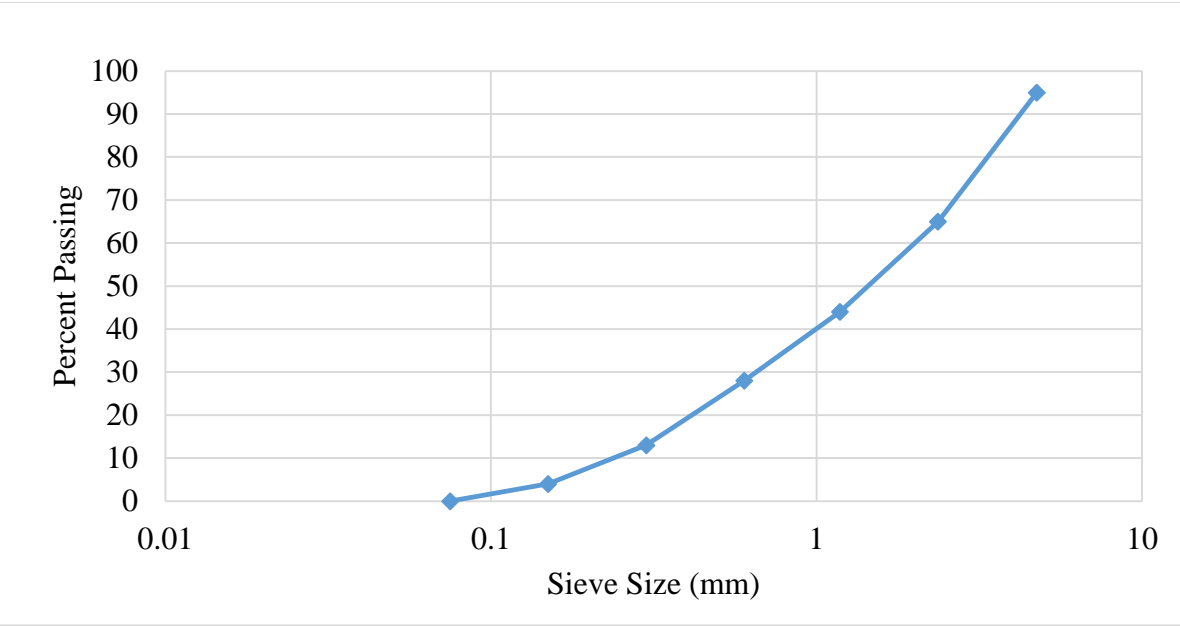
<b>Sieve No.</b>	<b>Sieve Size</b>	<b>Retained (gm)</b>	<b>Percent Retained</b>	<b>Cumulative Percent Retained</b>	<b>Percent Finer</b>
4	4.75	69.1	5.00	5	95
8	2.36	446.1	30.00	35	65
16	1.18	317.8	21	56	44
30	0.6	238.5	16	72	28
50	0.3	222.7	15	87	13
100	0.15	136.4	9	96	4
200	0.075	54.4	4	100	0
Pan	<0.0625	5	0	100	0

Figure 4.7 illustrates the gradation curve of open-graded bauxite aggregate used in this study. Almost 100% of the aggregate particles passed through the 4.75 mm sieve, and 98% were retained in the 1.19 mm sieve. Flint aggregate, however, is a densely graded aggregate (Figure 4.8) that includes a variety of particle sizes. In order to maintain the recommended gradation for high-

friction aggregate, particles that were retained on the 4.75 mm sieve and were finer than the 150  $\mu\text{m}$  sieve were discarded during the test. Use of particles finer than the 150  $\mu\text{m}$  sieve could prevent proper bonding between the aggregate and the epoxy.



**Figure 4.7 Gradation curve of bauxite aggregate**



**Figure 4.8 Gradation curve of flint aggregate**

#### 4.2.1.2 Specific gravity test results

Specific gravity is the ratio of the density of a unit weight of a substance to the density of unit weight of water. The specific gravity test was performed according to Kansas test method KT-6 in order to determine the dry and SSD bulk specific gravity of the aggregates. Table 4.3 shows specific gravity results of bauxite and flint aggregates. According to the test results, bauxite aggregate had higher dry and SSD bulk specific gravity than the flint aggregate.

**Table 4.3 Bulk specific gravity of bauxite and flint aggregate**

<b>Test performed</b>	<b>Bauxite</b>	<b>Flint</b>
Specific Gravity (Dry)	3.324	2.623
Specific Gravity (SSD)	3.327	2.638

#### 4.2.1.3 Moisture content test results

The moisture content test was performed according to Kansas test method KT-11 in order to determine the amount of moisture on aggregate surfaces. Since all aggregates are porous, moisture can be absorbed on the particles. According to high-friction particle specifications, aggregates can contain a maximum of 0.2% moisture. Results of the moisture content test showed that the bauxite aggregate had a moisture content of 10.5% and the flint aggregate had a moisture content of 15.6%. In order to eliminate excess moisture, both aggregates were dried completely in the oven, and then dried aggregates were used for the HFST process.

#### 4.2.1.4 Fine aggregate angularity test results

The FAA, or uncompacted void content test indirectly determines the angularity of fine aggregates. FAA determination is essential because excess rounded fine aggregate can lead to pavement rutting. Angular particles do not compact easily because their angular surfaces lock up with one another and resist compaction; rounded surfaces, however, try to pass by one another and

allow easier compaction. Therefore, the higher the measured uncompacted void content, the more angular the material. In this test, which was performed according to Kansas test method KT-50, FAA was determined by measuring the uncompacted void content of a sample. The FAA value was found to be 43 for bauxite aggregate and 48 for flint aggregate. As demonstrated by the test results, flint aggregate is more angular than bauxite aggregate.

#### **4.2.1.5 Sand equivalent test result**

The sand equivalent test of flint aggregate was performed according to AASHTO T 176 test procedures. Because flint aggregate contains an excessive amount of fine materials, the sand equivalent test was used to determine the relative proportions of fine dust or clay-like materials that can coat the aggregate and prevent proper binder-aggregate bonding. This test determined the clay and sand number, or the height of sand and clay after the aggregate was shaken, irrigated, and settled for a period of time. A higher sand equivalent value typically indicates a clean aggregate. The calculated sand number of the flint aggregate was found to be 78 which indicates that flint has lower portion of detrimental clay like particles.

#### **4.2.1.6 Durability index test result**

The DI value indicates relative resistance of an aggregate to produce detrimental clay-like fines when subjected to degradation. The minimum value of the DI should be 40 for 3 million Equivalent Single Axle Load. The DI of the flint aggregate was determined according to AASHTO D 3744 specifications. Test results showed that the DI value of flint aggregate was 42 which satisfies the required limit for 3 million ESAL.

### **4.2.2 Test Results of Prepared High-Friction Surfaces**

The following four sets of aggregate epoxy combinations were used in the lab to determine the performance of each set:

Combination 1: Bauxite aggregate and Mark-154 epoxy

Combination 2: Flint aggregate and Mark-154 epoxy

Combination 3: Bauxite aggregate and Pro-Poxy Type III epoxy

Combination 4: Flint aggregate and Pro-Poxy Type III epoxy

#### 4.2.2.1 Bauxite Aggregate-Mark-154 Epoxy Combination

For each combination, CTM readings were taken before and after application of HFSs and after testing with the HWTD. DFT readings were also taken before and after HFS application so that comparisons can be made. From CTM and DFT readings friction number of a given surface can be calculated. Figures 4.9 show CTM readings and figure 4.10 illustrate the improvement of friction number after application of HFSs prepared with bauxite aggregate and Mark-154 epoxy, respectively.

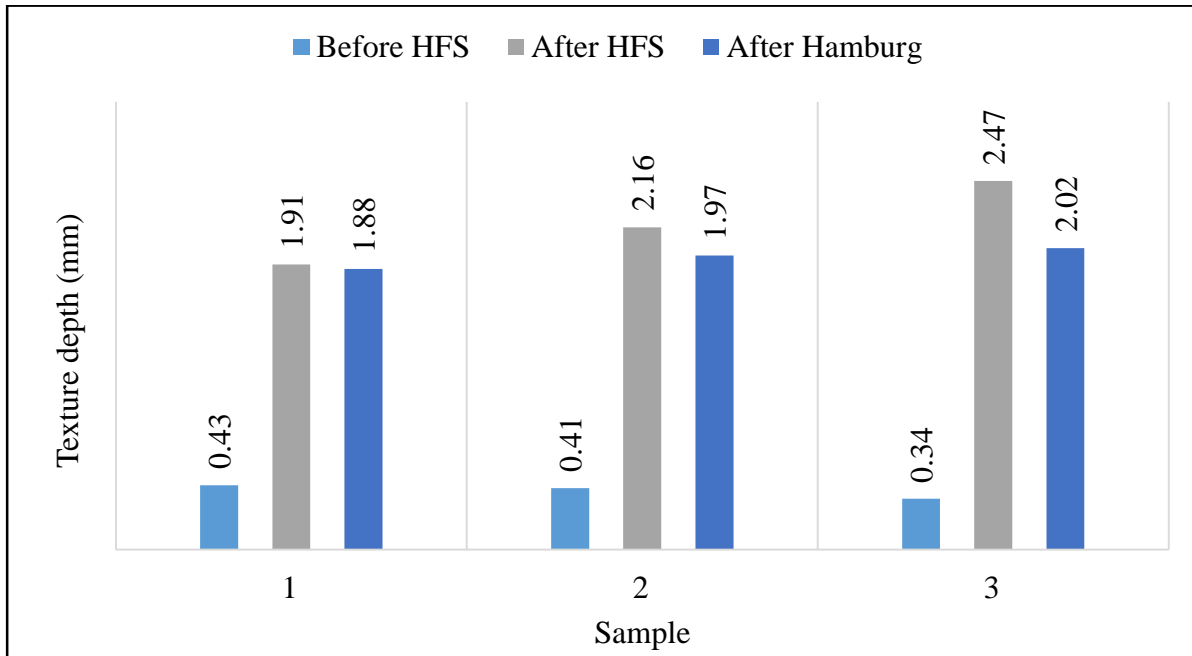
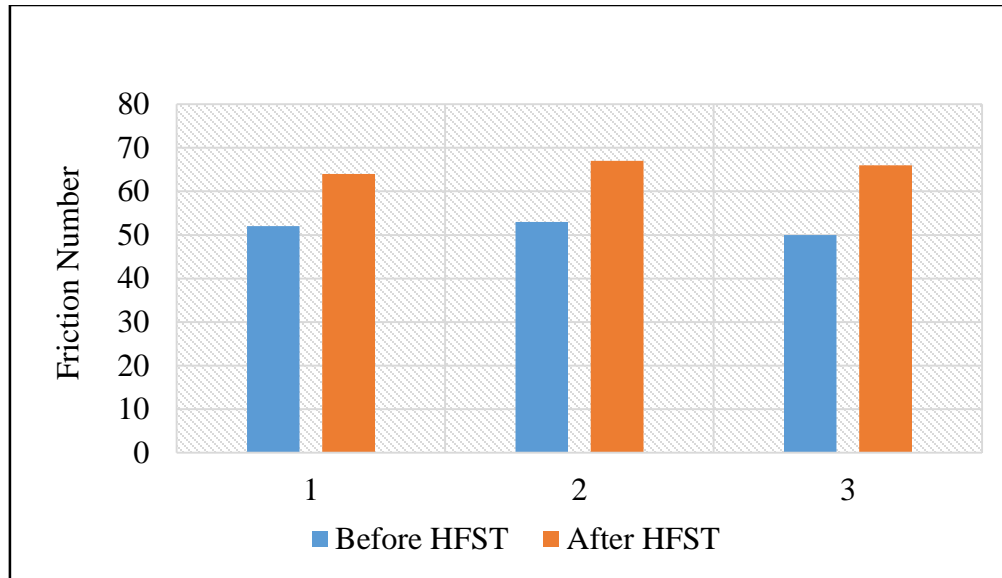


Figure 4.9 Texture depth of combination 1



**Figure 4.10 Improved FN of HFSs prepared with combination 1**

As shown in Figure 4.9, texture depth values of the bare slabs were very low before HFST application. Although HFST improved texture depth values significantly, texture depth decreased only slightly from previous values when the samples were tested with the HWTD. Figure 4.10 shows that the FN increased after HFST application. The FN varied from 50 to 53 before HFST but then varied from 64 to 67 after the treatment.

#### **4.2.2.2 Flint Aggregate-Mark-154 Epoxy Combination**

The combination 2 which is the high friction surface prepared with flint aggregate and Mark-154 epoxy demonstrated a similar pattern in texture depth and FN improvement, as shown in Figure 4.11 and Figure 4.12. Texture depth improved significantly after treatment, but texture depth demonstrated a greater increase than the previous aggregate-binder combination (combination 1). Similar to the previous combination, however, texture depth decreased after the HWTD test.

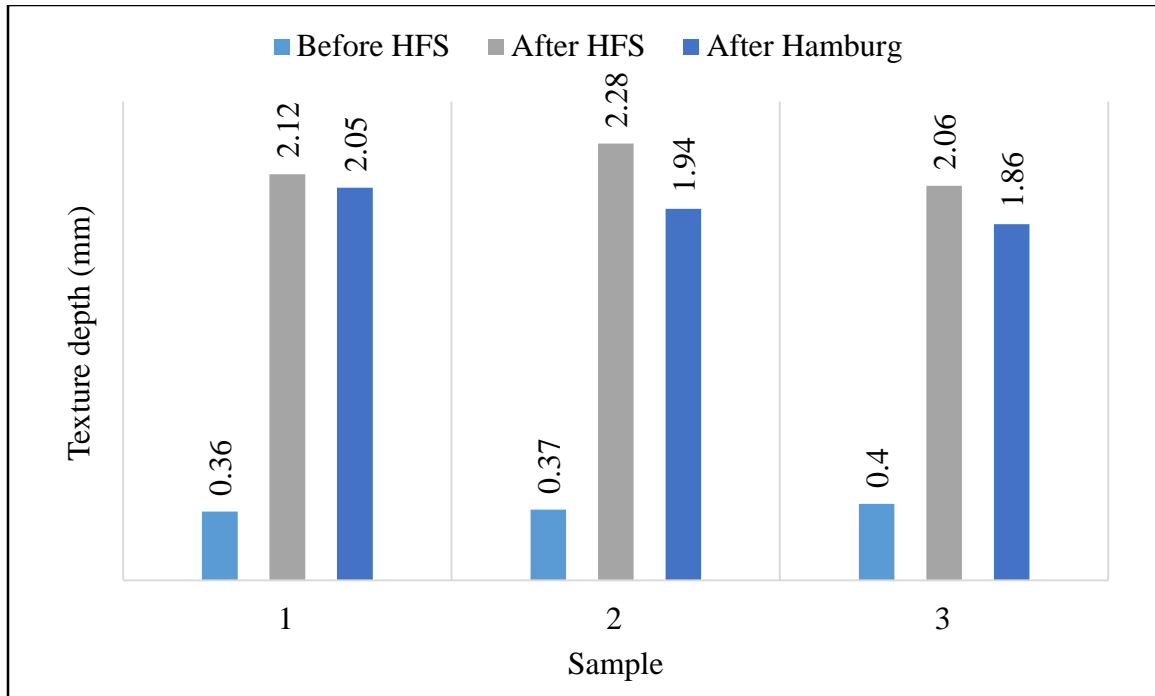


**Figure 4.11 Texture depth of combination 2**

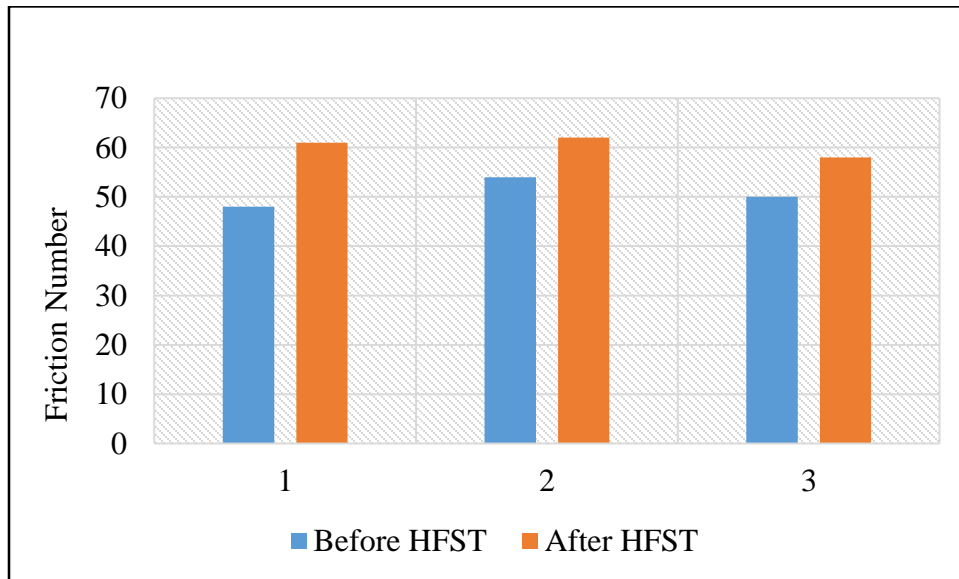


**Figure 4.12 Improved FN of HFSs prepared with combination 2**

Figure 4.12 shows that the FN increased after HFST application. The FN varied from 48 to 54 before HFST but then varied from 58 to 61 after treatment. Test results showed that the FN



of bauxite aggregate improved to 67 and increased to 62 for flint aggregate; friction improved by almost 150% in both cases.

#### 4.2.2.3 Bauxite Aggregate-Pro-Poxy Type III Epoxy Combination

The third aggregate epoxy combination consisted of bauxite aggregate and Pro-Poxy Type III epoxy. DFT malfunctions, however, prevented the acquisition of friction readings, so the FN for this aggregate binder combination could not be calculated. Only CTM readings were taken before and after HFST and after the HWTD test. Results are shown in Figure 4.13.

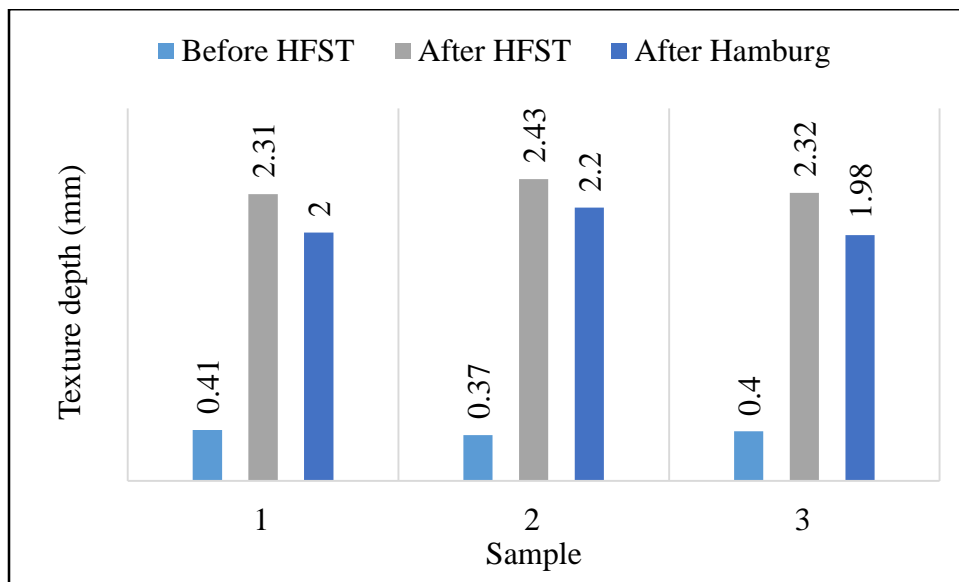


**Figure 4.13 Texture depth of combination 3**

This combination showed test results that were similar to the previous two combinations: Texture depth improved considerably after the treatment and after the HWTD test, and texture depth decreased only slightly. However, in this combination, texture depth reduction was lower after the HWTD test compared to the previous two combinations.

#### 4.2.2.4 Flint Aggregate-Pro-Poxy Type III Epoxy Combination

The fourth aggregate epoxy combination consisted of flint aggregate and Pro-Poxy Type III epoxy. DFT malfunctions prevented the determination of friction values for this aggregate

binder combination, thereby also preventing measurement of the FN. Only CTM readings were calculated before and after HFST and after the HWTD test. Results are shown in Figure 4.14.

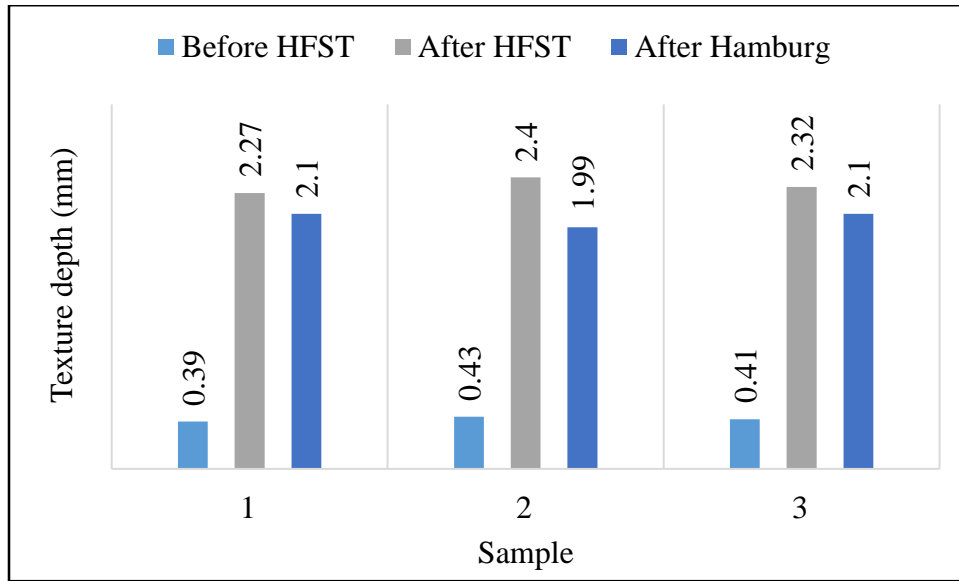


**Figure 4.14 Texture depth of combination 4**

A test pattern similar to the other three HFS combinations was observed, but the texture depth reduction after the HWTD test was lower than the first two combinations (combination 1 and 2). Test results showed that the use of Pro-Poxy Type III epoxy lowered ‘texture depth reduction’ after the HWTD test as compared to when Mark-154 epoxy was used. Therefore, Pro-Poxy Type III epoxy more effectively retained aggregates on high friction surfaces, resulting in less aggregate loss from the surface after traffic passes over the surfaces.

### 4.2.3 Statistical Analysis

Statistical analysis was performed to determine the effectiveness of HFST prepared with combination 1: bauxite aggregate and Mark-154 epoxy. The null hypothesis assumed that the FN improvement for this combination was not significant. A paired t-test was performed to compare the FN before and after the treatment. Using the experimental test results, calculated t-ratio was 12.12, where the t-critical value from the t-table was calculated to be 2.92 considering a 95%

confidence level. The calculated t-ratio, which was greater than the t-critical value, indicated rejection of the null hypothesis, which stated that the FN improves significantly when combination 1 is used for HFST.

HFST combination 2 consisted of flint aggregate and Mark-154 epoxy. Similar to combination 1, a paired t-test was performed to determine FN improvement for this combination. The calculated t-value was found to be 5.80, where the t-critical value from t-table was 2.92 according to a 95% confidence level. Therefore, the FN improved significantly with the combination of flint aggregate and Mark-154 epoxy.

A t-test was performed to determine whether the FN improvement differed significantly among combination 1 and 2 due to aggregate variation. Mark-154 epoxy was used for both cases. The null hypothesis stated that there was not significant difference of FN improvement among combination 1 and 2 due to change in the aggregate. Using the experimental test results, the t-value was calculated as 2.14, where the t-critical value from t-table was 2.92 according to a 95% confidence level. The  $t < t_{\text{critical}}$  value indicated acceptance of the null hypothesis, so no significant variation of FN improvement among combination 1 and 2 was evident due to aggregate changes. In other words, the use of Mark-154 epoxy caused similar FN improvement for both aggregates, indicating that flint aggregate can be used as an alternative to bauxite aggregate.

Statistical analysis was performed to determine the effectiveness of HFST prepared with a combination of bauxite aggregate and Pro-Poxy Type III epoxy. Due to malfunctioning of the DFT, however, FNs could not be measured. Therefore, in paired t-test, change of texture depths were considered as the responses instead of the FN improvement. The null hypothesis assumed that texture depth improvement after the treatment was not significant. A paired t-test was performed on slab specimens to compare texture depths before and after treatment. The calculated

t-ratio was 38.94, where the t-value from the t- table or the t-critical value was calculated to be 2.92 considering a 95% confidence level. The calculated t-ratio was greater than the t-critical value, indicating rejection of the null hypothesis, which stated that texture depth improves significantly after the treatment when combination 3 is used for HFST.

HFST combination 4 consisted of flint aggregate and Pro-Poxy Type III epoxy. Similar to combination 3, a paired t-test was performed to determine texture depth improvement after the treatment. Using experimental test results, he calculated t-value was found to be 72.57, where the t-value from t-table was 2.92 according to a 95% confidence level. Therefore, texture depth was shown to improve significantly after the treatment with a flint aggregate and Pro-Poxy Type III epoxy combination.

A t-test was performed to determine whether ‘texture depth improvement after treatment’ differ significantly among combination 3 and 4 due to aggregate variation. Pro-Poxy Type III was used in both cases. The null hypothesis stated that texture depth improvement does not change significantly among combination 3 and 4 due to change of aggregate. The t-value was calculated as 0.703, where the t-critical value from t-table was 2.92 according to a 95% confidence level. The  $t < t_{\text{critical}}$  value indicated acceptance of the null hypothesis, demonstrating no significant variation of texture depth improvement among combination 3 and 4 due to aggregate variation. In other words, use of Pro-Poxy Type III epoxy similarly improved texture depth for both aggregates, indicating that flint aggregate can be used as an alternative to bauxite aggregate.

Two-way factorial analysis was performed by constructing an Analysis of Variance (ANOVA) table. Factor 1 considered two levels, a) Mark-154 epoxy and b) Pro-Poxy Type III epoxy. Two levels also considered in factor 2, which are: a) bauxite aggregate and b) flint aggregate. Change of texture depth or CTM readings were considered as the responses in factored

analysis. Table 4.4 shows the results of the two-way factored analysis. In all the cases 95% confidence level was considered. Null hypothesis were:

- Epoxy has no significant effect on changing texture depth
- Aggregate has no significant effect on changing texture depth
- Epoxy and aggregate interaction has no significant effect on changing texture depth

**Table 4.4 Two-way factorial analysis result**

<b>Source of Variation</b>	<b>SS</b>	<b>df</b>	<b>MS</b>	<b>F</b>	<b>P-value</b>	<b>F critical</b>
Epoxy	0.075	1	0.075	2.276	0.169	5.317
Aggregate	0.001	1	0.001	0.056	0.817	5.317
Interaction	0.001	1	0.001	0.020	0.889	5.317
Within	0.264	8	0.033			
Total	0.342	11				

In all cases, calculated F-value was lower than the F-critical value. Thus null hypothesis could not be rejected. Thus, according to the statistical analysis test results, all epoxy-aggregate combinations showed similar texture depths.

## Chapter 5 - Conclusions and Recommendations

### 5.1 Conclusions

The objective of this research was to evaluate the performance of HFST using local aggregate instead of imported manufactured aggregate and also to observe the HFST performances on four Kansas highways. Before and after the treatment skid number and texture depth of the high friction surfaces were measured using a LWST and LCMS, respectively. In the laboratory, calcined bauxite and flint aggregates were used in this study in combination with Mark-154 and Pro-poxy Type iii epoxy. Aggregates were tested to determine gradation, specific gravity, moisture content, FAA, sand equivalent, and aggregate DI. A total of four aggregate epoxy combinations were tested in CTM, DFT, and HWTD. The following conclusions were drawn based on analysis results:

1. After HFST application, in-situ friction improved significantly in both laboratory and field.
2. De-bonding of high friction surfaces happened in the wheel path locations in some spots in KDOT highways.
3. In the laboratory, the gradation test indicated that bauxite is an open-graded aggregate and flint aggregate is densely graded. According to HFST specification, small aggregate particles could not be used because they prevent adequate aggregate binder bonding. Therefore, flint particles smaller than a 150  $\mu\text{m}$  sieve size and larger than a 4.75 mm sieve size were discarded during high friction surface preparation.
4. According to results of the specific gravity test, the dry and SSD specific gravities of the bauxite aggregate were slightly higher than the specific gravity of the flint aggregate.

5. Flint aggregate had higher moisture content than bauxite aggregate, so flint aggregate was washed over a No. 200 (75  $\mu$ m) sieve and dried in the oven to a constant mass in order to bring the moisture content within the required limit for an HFST aggregate.
6. The FAA, or uncompacted void content value of the flint aggregate was higher than the FAA value of the bauxite aggregate. It indicates that flint aggregate is more angular than bauxite and it is more resistant to compaction than bauxite aggregate.
7. Sand equivalent and aggregate DI values were calculated only for the flint aggregate. Results indicated that the percentage of detrimental clay or sand-like particle is very low in flint aggregate, proving that flint aggregate is an efficient alternative for HFST.
8. Statistical analysis of 'bauxite and Mark-154' combination and 'flint and Mark-154' combinations indicated no significant difference in FN improvement between the two aggregates. Therefore, flint aggregate can be used as an alternative to bauxite aggregate.
9. Statistical analysis of 'bauxite and Pro-Poxy Type III' combination and 'flint and Pro-Poxy Type III' combinations also showed no significant difference in texture depth improvement between aggregates, proving that flint can be used as an alternative to bauxite for HFST.
10. Two-way factored analysis of the four aggregate-epoxy combinations indicated that the variation of texture depth improvement was due to epoxy variations, not because of variations of aggregates. Results showed that Pro-Poxy Type III epoxy effectively retains an increased amount of aggregates on prepared HFSs than Mark-154 epoxy.
11. Texture depth improvement or skid resistance of flint and bauxite aggregate showed similar results, proving that HFST projects can increase cost-effectiveness by utilizing this local flint aggregate.

## **5.2 Recommendations**

Various complications arose during the test procedure. Wheel paths became smoother with time leading to the conclusion that pavement surface friction decreases after a certain number of traffic, requiring reapplication of HFST to increase friction. Further study is needed to solve this problem. In addition, HFST should be studied using other local hard aggregates in order to accurately indicate friction resistance properties of the aggregates and identify more durable and increasingly cost-effective options for HFST.



## References

- Baker, R. 2013. High Friction Surface Treatments: A Cost-Effective Strategy that Saves Lives, Newsroom, DBI services. Retrieved from, <http://www.dbiservices.com/news/high-friction-surface-treatments-cost-effective-strategy-saves-lives>.
- Baron, S. 2015. Preventing Vehicle Departures from Roadways, American Traffic Safety Services Association, pp. 12-13.
- Brimley, B., and Carlson, P. 2012. Using High Friction Surface Treatments to Improve Safety at Horizontal Curves, Texas Transportation Institute, The Texas A&M University System, pp. 15-16.
- Brown, E. R., Cooley, L. A., Hanson, Jr. D., Lynn, C., Powell, B., Prowell, B., and Watson, D. 2002. NCAT Test Track Design, NCAT Report No. 02-12, Construction and Performance, National Center for Asphalt Technology.
- Flintsch, G. W., De León Izeppi, E., McGhee, K. K., and Roa, J. A. 2009. Evaluation of the International Friction Index Coefficients for Various Devices, Transportation Research Record Journal of the Transportation Research Board 2094, pp 136-143.
- Hall, J. W., Smith, K. L., Wambold, J. C., Yager, T. J., and Rado, Z. 2009. Guide for Pavement Friction, National Cooperative Highway Research Program, Transportation Research Board of the National Academics, Contractor's Final Report for NCHRP Project 1-43, pp. 36-37.
- Henry J.J. 2000. Evaluation of Pavement Friction Characteristics, NCHRP Synthesis 291, National Cooperative Highway Research Program.
- High Friction Surface Treatment Overview. 2015. Florida Department of Transportation. Retrieved from, [tmp\\_1221\\_2-24-2015\\_100509\\_](http://tmp_1221_2-24-2015_100509_)

- High Friction Surfaces. 2014. Jointline Group Limited. Retrieved from, <http://www.jointline-group.co.uk/high-friction-surfaces.php>
- Hill, C. 2015. Pennsylvania DOT Co-hosts High Friction Surface Department demonstration, Equipment World's Better Roads. Retrieved from, <http://www.equipmentworld.com/pennsylvania-dot-co-hosts-high-friction-surface-treatment-demonstration/>
- Huhta, R. S., Meyer, D. A., and Zelnak, P. 2001. The Aggregate Handbook. Arlington, Virginia.
- Izeppi, E. L., Flintsch, G. W., and McGhee, K. 2010. Field Performance of High Friction Surfaces. Final Contract Report VRTC 10-CR6, Virginia Transport Research Council.
- Julian, F., and Moler, S. 2008. Gaining Traction in Roadway Safety, Public Roads, 72 (1). Retrieved from, <https://www.fhwa.dot.gov/publications/publicroads/08july/05.cfm>
- Kelly, T. 2008. Forensic Report of the Failure of Tyregrip, Materials Forensic Report, Florida Department of Transportation, Polk Parkway, Florida.
- Laurent, J., Lefebvre, D., and Samson, E. 2008. Development of a New 3D Transverse Profiling System for the Automatic Measurement of Road Cracks, 6th Symposium on Pavement Surface Characteristics.
- LeFante, J. 2015. High Friction Surfacing, Interstate Road Management. Retrieved from, [ftp://ftp.odot.state.or.us/Bridge/11\\_BR\\_MAINT\\_CONF\\_PDF/Session\\_2/2C\\_HFS\\_Br\\_Deck\\_Sealing\\_J\\_LeFante.pdf](ftp://ftp.odot.state.or.us/Bridge/11_BR_MAINT_CONF_PDF/Session_2/2C_HFS_Br_Deck_Sealing_J_LeFante.pdf).
- McGhee, K. K., Flintsch G. W., and de Leon Izeppi, E. 2003. Using High-Speed Texture Measurements to Improve Uniformity of Hot-Mix Asphalt. VTRC 03-R12, Virginia Transportation Research Council.

- Meggers, D. 2015. Evaluation of High Friction Surface Locations in Kansas, Transportation Research Board 94th Annual Meeting, Washington, D.C., USA.
- Merritt, D. K., Lyon, C. A., and Persaud, B. N. 2015. Evaluation of Pavement Safety Performance, Report No. FHWA-HRT-14-065, Turner-Fairbank Highway Research Center, pp. 109.
- Micro Surfacing and Slurry Seal. 2015. The Gorman Group, LLC. Retrieved from, <http://www.gormanroads.com/micro.php>.
- Mills, J. 2015. Benefit- Cost Analysis of Florida High-Friction Surface Treatments, TRB 95<sup>th</sup> Annual Meeting. Retrieved from, <http://www.slideshare.net/TTITAMU/benefitcost-analysis-of-florida-highfriction-surface-treatments>.
- Nicholls, J. C. 1997. Laboratory Tests on High-Friction Surfaces for Highways, Report 176, Transportation Research Laboratory.
- Nicholls, J. C. 1998. Trials of High-Friction Surfaces for Highways, Report 125, Transportation Research Laboratory.
- Peshkin, D., Smith, K. L., Wolters, A., Krstulovich, J., Moulthrop, J., and Alvarado, C. 2011. Preservation Approaches for High-Traffic-Volume Roadways, Transportation Research Board, pp. 97-98.
- Rajagopal, A. 2010. Effectiveness of Chip Sealing and Microsurfacing on Pavement Serviceability and Life, Final Report, Ohio DOT and FHWA, pp. 47-48.
- Rao, T.V. 2003. Metal Casting: Principles and Practice, New Age International, ISBN 978-81-224-0843-0, pp. 110-111.
- Reddy, V., Datta, T., Savolainen, P., and Pinapaka, S. 2009. A Study of the Effectiveness of Tyregrip High Friction Surface Treatment, Accident Reconstruction Journal, 19 (5), pp. 53-57.

- Shi, C. 2004. Steel Slag: Production, Processing, Characteristics, and Cementous Properties, *Journal of Materials in Civil Engineering*, 16 (3), pp. 230-236.
- Sorrell, C. A. 1973. *Minerals of the World: A Field Guide and Introduction to the Geology and Chemistry of Minerals*, Golden Press, New York, pp 206–209.
- Stoikes, J. 2014. Get a Grip, *Asphalt Contractor Magazine*. Retrieved from, <http://www.forconstructionpros.com/article/11576932/high-friction-surface-treatments-add-grip-to-roads-saving-money-and-lives>
- Viner, H. E., Parry, A. R., and Sinhal, R. 2005. Linking Road Traffic Accidents with Skid Resistance: Recent UK Development, *International Conference on Surface Friction of Roads and Runways*.
- Wallman, C. G., and Astrom, H. 2001. *Friction Measurement Methods and the Correlation between Road Friction and Traffic Safety: A Literature Review*, Swedish National Road and Transport Research Institute, pp. 42.
- Wambold, J. C. 1988. Obtaining Skid Number at Any Speed from Test at Single Speed, *Transportation Research Record Journal of the Transportation Research Board* 1196, pp. 300-305.
- Wang, G., Morian, D., and Frith, D. 2013. Cost-Benefit Analysis of Thin Surface Treatments in Pavement Treatment Strategies and Cycle Maintenance, *Journal of Civil Engineering*, American Society of Civil Engineers, 25 (8), pp. 1050–1058.
- Zahir, H., Hossain, M., and Miller, R. 2015. 3-D Laser Data Collection and Analysis of Road Surface Texture, *Road Profile User’s Group Meeting*, Raleigh, NC.